Ph.D. degree in Systems Medicine
(Curriculum in Human Genetics)
XXX cycle, Settore disciplinare: Med/04

European School of Molecular Medicine (SEMM)

University of Milan and University of Naples "Federico II"

Role of JNK and CHOP in the pathogenesis of liver disease due to Z alpha-1 antitrypsin

Author
Sergio Attanasio
TIGEM, Naples
Matricola: R11119

Supervisor

Prof. Nicola Brunetti-Pierri (TIGEM, Naples)

Internal advisor:

Prof. Carmine Settembre (TIGEM, Naples)

External advisor:

Prof. Maria Elena Banos Miranda (University of Rome "La Sapienza")

Anno accademico 2017-2018

Table of Contents

List of figures

List of tables

List of abbreviations

AAT	Alpha-1 antitrypsin
AATD	Alpha-1 antitrypsin deficiency
ALT	Alanine aminotransferase
AP-1	Activator protein 1
ATZ	Z alpha-1 antitrypsin
BAP31	B cell receptor associated protein 31
BiP	Binding immunoglobulin protein
bZIP	Basic-leucine zipper
C/EBPβ	CCAAT Enhancer Binding Protein Beta
ChIP	Chromatin immunoprecipitation
CHOP	CCAAT/Enhancer-Binding Protein Homologous Protein
COPD	Chronic obstructive pulmonary disease
CRE	cAMP-responsive element
DDIT3	DNA damage inducible transcript 3
ER	Endoplasmic reticulum
ERAD	ER-associated degradation pathway
ERK	Extracellular signal-regulated kinase
FXR	Farnesoid X receptor
HCC	Hepatocellular carcinoma
HNF1	Hepatocyte nuclear factors 1
HNF3	Hepatocyte nuclear factors 3
IL1β	Interleukin 1β
IL6	Interleukin 6
JNK	c-JUN N-terminal kinase
MAPK	Mitogen-activated protein kinase
NE	Neutrophil elastase
NFκB	Nuclear factor κb
OSM	Oncostatin M
PAS-D	Periodic acid Schiff-diastase resistant
RCL	Reactive central loop
TFEB	Transcription factor EB
TNFα	Tumor necrosis factor-α
TRE	Phorbol 12-O-tetradecanoate-13-acetate (TPA)-responsive element
UPR	Unfolded protein response
UPS	Ubiquitin proteasome system
UTR	Untranslated region

Chapter 1: Abstract

Alpha-1 antitrypsin (AAT) deficiency is a genetic disease that can affect both the lung and the liver. The vast majority of patients harbor a mutation in the *SERPINA1* gene resulting in a single substitution from glutamic acid to lysine at amino acid position 342 (p.E342K). The AAT encoded by the Z allele (ATZ) is not properly folded and accumulates in the endoplasmic reticulum (ER) of hepatocytes resulting in liver disease through a gain of function mechanism. The liver disease is a prototype of conformational disorder due to protein misfolding and aggregation. Intracellular retention of ATZ triggers a complex injury cascade including autophagy, ER-stress and other mechanisms. Nevertheless, several aspects of the disease pathogenesis are still unclear.

I found that ATZ induces activation of c-JUN N-terminal kinase (JNK) and c-JUN signaling in livers of a mouse model (PiZ mice) of the disease. JNK activation was confirmed in human livers of patients homozygous for the Z allele with severe liver disease requiring hepatic transplantation. In mice, genetic ablation of *Jnk1* or *Jnk2* decreased ATZ levels by reducing c-JUN mediated *SERPINA1* expression. Moreover, I have found up-regulation of genes associated with response to ER stress in PiZ mouse livers by expression array profiling. Among the differentially expressed genes, I focused on the *CCAAT/Enhancer-Binding Protein Homologous Protein* (*Chop)* that was significantly up-regulated in both mouse and human livers expressing ATZ. To investigate the role of CHOP in ATZ-induced liver damage, I crossed PiZ with *Chop* null ($Chop^{-/-}$) mice. Genetic ablation of *Chop* resulted in a marked reduction of hepatic ATZ levels in juvenile PiZ mice. *SERPINA1* mRNA levels in livers of PiZ/$Chop^{-/-}$ mice were also significantly reduced compared to PiZ controls, suggesting that CHOP induces ATZ accumulation by increasing *SERPINA1* transcription. CHOP was indeed found to up-regulate *SERPINA1* expression through binding with C/EBPβ and c-JUN on *SERPINA1* regulatory elements. So far, JNK and CHOP have been involved in the pathogenesis of several liver disorders

but not in hepatic disease induced by ATZ. The results of my studies show that JNK and CHOP are important players in the disease pathogenesis and are novel therapeutic targets.

Chapter 2: Introduction

2.1 Alpha-1 antitrypsin deficiency

Alpha1-antitrypsin (AAT) deficiency (AATD, OMIM #613490) is an inherited disorder that may result in lung and liver disease [1]. It was described for the first time in 1963 by Laurell and Eriksson which observed the lack of alpha-1 band on serum protein electrophoresis of individuals with severe obstructive lung disease [2]. The association with liver disease was reported in the 1969 by Sharp and colleagues who observed familial infantile liver cirrhosis in patients with AATD [3]. The disorder is inherited by an autosomal codominant pattern and affects about 1 in 2,000-3,000 live births [4, 5]. However, the prevalence varies among populations with higher frequency in individuals of European ancestry and lower frequency in people of Asian descent [6]. Nevertheless, AATD is largely under diagnosed and exact prevalence in most populations remains unknown [7].

2.1.1 Clinical manifestations

Signs and symptoms of the disease and their onset vary among individuals. The most frequently affected organs are lung and liver, while the skin is less frequently involved. Patients with AATD develop the first signs and symptoms of lung disease between the third and fourth decades of life [8]. The classic symptoms at the onset are shortness of breath following mild physical activity, wheezing, and increased risk of lung infections [8]. Affected individuals often develop chronic obstructive pulmonary disease (COPD) and panlobular lung emphysema [9]. Moreover, the lung of subjects with AATD showed an increased inflammation, associated to increased neutrophils and cytokines levels (especially leukotriene B4; LTB4) [10, 11]. Smoking or exposure to tobacco smoke accelerates the damage to the lungs and the onset of emphysema. In addition to increasing the inflammatory reaction in the respiratory tract, cigarette smoke directly inactivates AAT by oxidizing essential methionine residues to sulfoxide forms, and thus decreasing the

enzyme activity [12]. Other symptoms may include chronic bronchitis or bronchiectasis [13].

The spectrum of liver disease varies enormously and it includes asymptomatic states, acute liver failure, fibrosis, cirrhosis and increased risk of developing hepatocellular carcinoma (HCC) [14]. Liver biopsy findings in both children and adult patients may include steatosis and lobular inflammation. Analysis of a unique cohort of homozygotes identified by an unbiased newborn screening performed in Sweden has shown that about 8% of homozygotes develop clinically significant liver disease in the first four decades of life [15, 16], indicating that genetic and/or environmental modifiers play a major role in susceptibility to liver disease. So far, a single nucleotide polymorphism that suppresses the translation of a protein involved in ER-associated degradation pathway (ERAD), ERManI, was found to accelerate the onset of end-stage liver disease [17]. Clinical data indicate that there are two pick ages for severe AATD-associated liver disease to present: birth to 5 and 50-65 years of age [18]. Moreover, the human disease has different features in infants compared to adults. These differences suggest that pathogenic mechanisms vary depending on the age and more powerful modifiers play a role in the liver disease in children.

In rare cases, patients affected by AATD develop a skin condition named as panniculitis [19], presenting with painful, weepy cutaneous nodules that can sometimes undergo to necrosis. Vasculitis is another of the rare skin manifestations associated to AATD [20].

Measurement of serum AAT concentration is the first step in the diagnosis of AATD. A reduction of 50% of the lower limit of the normal range in serum levels of AAT is considered an evidence for AATD. However, AAT levels can increase several folds in response to different conditions, thus making difficult to detect its deficiency [21]. A more definitive and specific diagnostic method is the genotype analysis by polymerase chain reaction (PCR) and sequencing of the PCR products. Nevertheless, many individuals with AATD are likely undiagnosed [7] because several affected subjects are asymptomatic or have delayed onset of symptoms. Thus, the diagnostic tests should be performed for all

patients with liver disease of unexplained etiology and those with COPD and asthma showing resistance to medical therapy. Moreover, once an index case has been diagnosed, it is strongly recommended to test all at the risk relatives.

2.1.2 Genetics and polymorphisms of *SERPINA1*

AAT is encoded by *SERPINA1* gene, also known as the protease inhibitor (Pi). Mutations in the *SERPINA1* gene can cause AATD. So far, more than 100 variants have been identified and the different AAT variants are distinguishable by isoelectric focusing [22]. The migration phenotype of mature, glycosylated wild type protein was denoted M, and homozygotes classified as PiMM. Other variants that migrate slower or faster are termed A-L and N-Z, depending on whether they run proximal or distal to the M band. The most common severe deficiency variant migrates the slowest and is named Z [23]. Some of these variants do not affect production of AAT while others cause deficiency of the protein with clinically significant effects. On the basis of plasma levels and function of AAT, variants are classified as normal, deficient, null and dysfunctional. Thus, the levels of AAT in the serum depend on the genotype. In circulating plasma of normal PiMM subjects, AAT concentration is in the range of 20-50 μM. Deficient alleles are associated with lower plasma AAT levels. The most common deficiency variant is produced by Z allele (p.E342K) followed by the S allele (p.E264V). Individuals homozygous for the S allele (PiSS) have a mild reduction in serum AAT levels whereas PiZZ subjects with two copies of the Z allele (ZZ) in each cell have a severe reduction in serum AAT levels, which are decreased to 10-15% of the normal levels. Those with the SZ combination have an increased risk of developing lung diseases (such as emphysema), particularly if they smoke. Individuals with an MS combination usually produce enough AAT to protect their lungs. People with MZ alleles, however, have a slightly increased risk of impaired lung or liver functions. The dysfunctional variants, such as the Pittsburgh variant (p.M358R) [24], have altered protein function and are synthesized in normal quantities. These variants lead

to reduced anti-proteases inhibition and are thus associated with lung disease. The null alleles, like the null-Hong Kong allele [25], produce no detectable AAT protein in the plasma and are associated with only lung disease but not the liver disease and high risk to develop COPD.

2.1.3 AAT: gene regulation, structure and function of the protein

SERPINA1 gene is approximately 12.2 Kb in size on chromosome 14q32.13 [26] and is composed by seven exons and six introns. First three exons are transcriptionally alternative and termed as 1A, 1B, and 1C [27]. Different tissue-specific isoforms are generated mainly by the usage of different transcription starting sites (TSS) and also through alternative splicing, thus reflecting the important of 5'untranslated region (UTR) in the regulation of *SERPINA1* expression. The hepatic TSS is located within the exon 1C while the TSS in monocytes is positioned in the exon 1A [28]. The Exon 2 contains the translational starting site for all the isoforms, producing a protein of 418 amino acids, including a 24 amino acids signal sequence. The regulation of the gene expression is mainly transcriptional and tissue-specific. Trans-acting factors, including Hepatocyte nuclear factors 1 (HNF1) and 3 (HNF3), are able to bind *SERPINA1* promoter and thereby, they contribute to its expression in the liver [29]. In addition, *SERPINA1* gene has enhancer regulatory regions located at 5'UTR that contains putative binding sites for the Activator protein 1 (AP-1) family of transcription factors (including members of JUN, FOS and ATF families) and the CCAAT Enhancer Binding Protein Beta (C/EBPβ) [30].

AAT is an acute phase protein and its blood levels typically increase by 2- to 4-folds during inflammatory responses [31]. Moreover, expression of *SERPINA1* is controlled by several cytokines such as interleukin 6 (IL6), interleukin 1β (IL1β), oncostatin M (OSM), and tumor necrosis factor-α (TNFα) [32].

AAT is a 52-kDa glycoprotein synthesized mainly by hepatocytes in the liver [33, 34]. However, other cell types can produce AAT, including lung and gut epithelial cells [35-

37], neutrophils [38], and alveolar macrophages [39]. During its synthesis, AAT is targeted to the endoplasmic reticulum (ER) to be folded and glycosylated at three distinct asparagine residues (amino acid residues 46, 83, and 247). The protein is further processed in the Golgi and, then, secreted into the blood.

AAT is a serine protease inhibitor protein and its key function is to inhibit neutrophil elastase (NE) within the lung [40]. During infections, NE is released from white blood cells to fight infections, but it can also attack normal tissues (especially the lungs) if not tightly controlled by anti-proteases such as AAT. In addition to NE, AAT can also inhibit other proteases such as trypsin, cathepsin G, and proteinase 3 [41]. AAT shares both structural and functional characteristics with other members of the serpin family including alpha-1 anti-chymotrypsin, protein C inhibitor, and anti-thrombin III. It is composed by three beta-sheets (named from A to C) and nine alpha-helices (named from A to I). The active site is located at the amino acids Met358-Ser359, which are part of a reactive center loop. Upon binding, serine proteases cleave the Met358-Ser359 bond releasing potential energy and resulting in a conformational change leading to protease distortion and inactivation. The resulting AAT-protease complex is then recognized by hepatic receptors and removed from circulation [42].

AAT has also anti-inflammatory and immunomodulatory functions. For example, AAT reduces neutrophil chemotaxis [43], inhibits TNFα and cytokines release from monocytes and neutrophils in response to endotoxin [44-47].

2.1.4 Pathobiology of AATD

Different mutations in the *SERPINA1* gene have been described. However, most of patients with AATD (about 95%) are homozygous for the Z allele, which is a single amino acid substitution at position 342 changing glutamic acid into lysine (p.E342K). This mutation alters protein folding and causes polymerization of mutant Z alpha-1 antitrypsin (referred as ATZ) in the endoplasmic reticulum (ER) [48]. In PiZZ individuals

homozygous for the Z allele, AAT levels in the serum are less than 15% of normal, due to its retention in the ER. The low circulating levels of AAT lead to an inadequate anti-protease protection in the lower respiratory tract that might lead to progressive lung emphysema. PiZZ individuals are also at risk of developing liver disease due to intracellular retention and accumulation of aberrantly folded and proteotoxic ATZ in hepatocytes that might lead to hepatitis, fibrosis, cirrhosis, liver failure, and HCC [49]. Therefore, the lung disease is caused by a loss of AAT function while the liver disease is due a gain of function mechanism.

The pathogenesis of HCC due to accumulation of ATZ is still poorly understood. One possible mechanistic explanation arises from the evidence that only a proportion of hepatocytes have intracellular ATZ globules in the livers of PiZZ patients. This observation suggests that globule-containing hepatocytes can produce regenerative signals acting on globule-devoid hepatocytes which in turn acquire a proliferative advantage and can develop cancer [50]. However, this hypothesis has to be confirmed and signaling pathways involved in cancer onset and progression have not been yet identified.

2.1.5 Mechanism of ATZ polymerization

Misfolding and polymerization are central features in the pathogenesis of AATD. Several pathogenic variants of AAT were found to cause intracellular polymerization and plasma deficiency. In addition, mutations in other members of the serpin family also resulted in protein aggregation, e.g. thrombosis due to anti-thrombin aggregation, angioedema due to aggregation of C1 inhibitor and encephalopathy due to neuroserpin aggregation. Because a common mechanism is involved in polymerization of these different proteins, these diseases are also defined as serpinophaties [51]. Understanding of the structural mechanism responsible for ATZ polymerization is therefore important to prevent AATD and possibly other disorders.

Different models of AAT polymerization have been proposed and they are based on different conditions giving rise to structurally and dynamically different polymer species. According to the first model proposed by Lomas and colleagues in 1992 and known as "single-strand linkage", the polymerization occurs through linkage by the incorporation of a portion of the reactive central loop (RCL) of one monomer into the β-sheet A of another monomer [48]. This model was supported by the evidence that exogenous RCL peptides block polymerization. However, two alternative models have also been proposed. One model known as "β-harpin linkage" is based on crystal structure of a dimer of anti-thrombin in which the intermolecular linkage included the insertion of two long β-strands (s4A and s5A) of one molecule into β-sheet A of another [52]. The last model, known as "triple-strand linkage", was extrapolated by the crystal structure of a self-terminating trimer of AAT [53]. The intermolecular linkage consists of the three C-terminal β-strands of AAT. Self-terminating trimer is recognized by the 2C1 antibody, which recognizes polymers from the liver of subjects affected by AATD [54]. These data suggest that single and/or triple-strand linkage may induce disease-relevant polymerization.

2.1.6 Intracellular processing of ATZ

Disposal of proteotoxic ATZ is mediated by two major pathways: ubiquitin proteasome system (UPS) and autophagy. It has been estimated *in vitro* that approximately 70% of ATZ is degraded by the proteasome through the ER-associated degradation (ERAD) pathway, 15% is normally secreted into the blood while the remaining 15% forms polymers within the ER. ATZ polymers are in part degraded by autophagy, but a proportion persists in insoluble inclusions [55].

The ER-associated degradation (ERAD) pathway is a highly conserved process by which folding-defective proteins are selected and ultimately degraded by the proteasome. The ERAD substrates are recognized in the ER and then ubiquitinated and dislocated from ER to the cytosol for proteasome degradation. Currently, the complex involved in the

dislocation of proteins from the ER to the cytosol remains unkown. Several candidates have been suggested including the Derlins (Derlin 1-3), Sec61, and the E3 ubiquint ligase HRD1 [56]. Recent studies showed that HRD1 is involved in the dislocation of both null Hong Kong variant and ATZ leading to their degradation in the cytosol by proteasome [57, 58].

Autophagy is a ubiquitous catabolic process by which cells digest their internal constituent to generate amino acids in response to nutrient starvation and other stimuli. It is characterized by the formation of double-membrane vesicles in the cytoplasm, which sequester cytoplasm and subcellular organelles and then fuse with lysosomes for degradation of its contents [59]. The autophagic pathway has been shown to play a crucial role in the degradation of aggregated proteins, and defects in autophagy have been implicated in the pathogenesis of several degenerative diseases [60]. Autophagy was first implicated in AATD when abundant autophagosomes were observed in mammalian cells expressing ATZ, in livers of PiZ mice and in livers of patients with AATD [61]. Further evidence for the role of autophagy in disposal of ATZ was provided by *in vitro* studies showing delayed degradation of ATZ in mammalian cell lines and in yeast strains with deficient autophagy [62, 63]. Studies in a mouse model engineered to express ATZ under the control of a liver specific and inducible promoter showed that accumulation of ATZ is sufficient to activate autophagy [62]. In yeast which are autophagy-deficient by a mutation in ATG6 (beclin 1 in mammals), ATZ disposal is only impaired at high levels of expression [63]. Recent evidences showed that a novel ER-to-lysosome-associated degradation (ERLAD) pathway different from canonical autophagy could be responsible for degradation of proteasome-resistant polymers of ATZ. According to this model, degradation of ATZ occurs via receptor-mediated vesicular transport [64].

Taken together, these results suggest that the ERAD/proteasomal pathway can handle ATZ at lower levels of expression, presumably because it is capable of degrading

soluble forms of ATZ, but when the expression is higher and ATZ accumulates in polymers and insoluble aggregates, autophagy becomes critical for ATZ degradation.

2.1.7 Pathways affected by ATZ in the liver

Several signaling pathways are specifically activated in response to intracellular ATZ accumulation in the ER. Such responses are relevant because they could potentially aggravate or protect from the liver damage induced by ATZ. Notably, in cell lines ATZ induces activation of B cell receptor associated protein 31 (BAP31), involved in ER quality control, and the nuclear factor κb (NFκB) [65]. Activation of NFκB has important implications because it mediates inflammation in the liver. Furthermore, NFκB plays a role in the liver carcinogenesis [66]. Moreover, ATZ accumulation results in caspase activation and mitochondrial injury [67] and induces accumulation of polyubiquitinated conjugates like in other disorders with protein aggregation [68].

Although its role in the pathogenesis of AATD has been suspected, the involvement of the unfolded protein response (UPR) remains still controversial. Terminally truncated variants of AAT (e.g. Null-Hong Kong and Saar AAT) constitutively activate the UPR [69, 70]. In contrast, misfolded ATZ in both cell lines and transgenic mice does not activate the UPR, even if this pathway is still functional [65, 70]. However, evidences supporting activation of the UPR have been generated in human lung epithelial and liver cells from PiZZ patients [71, 72] and in different cell lines by association of ATZ with chaperones, including binding immunoglobulin protein (BiP) [73].

Recently, our group reported that intrahepatic accumulation of ATZ has broad effects on metabolic liver functions, by affecting liver zonation, HNF4α and β-catenin signaling [74].

In summary, although several pathways have been shown to affect AATD-related liver disease, the mechanisms underlying hepatocyte damage and the increase risk of cirrhosis and HCC due to ATZ are not completely understood.

In this PhD thesis I investigated pathways involved in the pathogenesis of liver disease due to ATZ with the goal of identifying therapeutic targets for treatment of the AATD-related liver disease.

2.1.8 Therapeutic treatment approaches

Prevention of both lung and liver diseases is extremely important in AATD patients. Avoiding cigarette smoking and alcohol intake are extremely important to prevent or delay the development of lung and liver diseases. The mainstay of treatment for severe AATD is the AAT augmentation (replacement) therapy, that is the only specific non-invasive treatment for AATD able to correct the anti-elastase deficiency [75]. However, AAT augmentation therapy has no effect on the liver disease. AAT has been purified from the plasma of healthy individuals and delivered intravenously to patients at the dose of 60mg/kg body weight on a weekly basis. This treatment raises levels of serum AAT above the threshold of 11μmol/L that is considered to be protective [76]. Augmentation therapy indeed results in reduction of the frequency of respiratory tract infections and a decline in markers of inflammation. Alternative route of administration have also been investigated. Delivery by inhalation was found to be effective. Moreover, several recombinant forms of AAT (rAAT) are being developed although none of such recombinant proteins have yet approved for human use. In addition, these recombinant proteins are cleared rapidly from the circulation likely because they have different glycosylation patterns compared to the AAT made by the human liver, affecting their blood half-life [77, 78].

Gene therapy has also been investigated for the treatment of lung disease of AATD. This approach is based on gene transfer of AAT to muscle cells by multiple intramuscular injections and it has been investigated in clinical trials [79-81]. Although the injections were well tolerated by patients and no serious adverse events were reported, these clinical trials failed to show blood levels of AAT above the protective threshold of 11 μM [79-81].

Because this approach is based on ectopic expression of AAT by muscle cells, it does not address the liver disease of AATD.

So far protein augmentation therapy represents the only approved therapy for AATD and lung transplantation is the only available option for subjects with severe airflow obstruction and emphysema.

Currently, there are no drug-based therapies for the liver disease. As mentioned earlier protein augmentation has no effect on the liver disease that is due a gain of function mechanism. Severely affected can only be treated with orthotropic liver transplantation. However, we and others believe that a deep understanding of the mechanism underlying the disease pathogenesis have potential to unravel novel and more specific *druggable* targets. One strategy is to increase disposal of ATZ by stimulating autophagy using small molecules (e.g., carbamazepine and rapamycin) [82, 83] or gene transfer of the autophagy regulator transcription factor EB (TFEB) [84]. These approaches have been investigated at the preclinical level in a mouse model of AATD and have shown promising results in terms of reduction of intracellular ATZ and reduced hepatic fibrosis. One of such studies has been translated into a clinical trial investigating the efficacy of carbamazepine in patients with severe liver disease (ClinicalTrials.gov Identifier: NCT01379469).

Other approaches aim to block intracellular ATZ polymerization or to increase the folding and the secretion of the mutant ATZ by using small molecules and molecular chaperones [85-88]. In addition, RNA interference (RNAi)-based approaches to silence ATZ expression in the hepatocytes have been investigated in preclinical models and in clinical trials [89, 90]. Although these therapeutic approaches showed promising results in mice and non-human primates at reducing ATZ levels and preventing liver fibrosis, they are currently on hold because of potential safety concerns [91]. In conclusion, liver disease due to ATZ is still lacking non-invaside therapies and their development is urgently needed.

Chapter 3: Materials and methods

3.1 Mouse studies

Mouse procedures were performed in accordance to regulations of the Italian Ministry of Health. PiZ transgenic mice [92] were maintained on a C57BL/6 background. *Jnk1*$^{-/-}$ [93], *Jnk2*$^{-/-}$ [94], and *Chop*$^{-/-}$ [95] mice were purchased from Jackson laboratory and bred with PiZ mice. As positive controls of CHOP activation, C57BL/6 (Charles River Laboratories) mice were treated with DMSO (Sigma) or Tunicamycin (Sigma) 4 μg/g for 24 hours by intra-peritoneal injection. Tunicamycin is a small molecule which inhibits N-linked glycosylation leading to endoplasmic reticulum (ER)-stress and activation of CHOP. As positive controls of TUNEL staining, C57BL/6 (Charles River Laboratories) mice were treated with 5 μg/g of body weight of CD95-activating antibody for 6 hours. CD95 is a cell death receptor of the TNFR superfamily that induces apoptosis. rAAV8pCB-mir914-GFP and rAAV8pCB-GFP were generated, purified, and tittered by the UMass Gene Therapy Vector Core as previously described [96]. Vectors were diluted in saline solution and intravenously injected in 4-week-old PiZ mice at the dose of $1x10^{13}$ genome copies (gc)/Kg. Only male mice were used for all experiments. Blood samples were collected by retro-orbital bleedings and were analyzed for alanine aminotransferase (ALT) levels by fluorometric assay kit (Biovision) according to manufacturer's instructions using 1 μL of mouse serum, for each well, diluted in the buffer provided by the kit.

3.2 Liver staining and analyses

For immunofluorescence and histological analysis, liver specimens were fixed in 4% paraformaldehyde (PFA) overnight at 4°C. After three washes with phosphate-buffered saline (PBS), samples were dehydrated and then embedded into paraffin.

Periodic-acid Shiff diastase resistant (PAS-D) staining was performed on 6μm-thick sections of mouse and human livers. This staining marks the glycoprotein, allowing the

visualization of ATZ globules in pink. Sections were rehydrated and treated with amylase (Sigma) 0.5% for 20 minutes at room temperature (RT) and then stained with PAS reagent according to the manufacturer's instructions (Bio-Optica). Stained liver sections were examined under a Leica DM5000 microscope.

Sirius red staining was performed on 6µm-thick liver sections to mark collagen fibers and evaluate hepatic fibrosis. Sections were rehydrated and stained for 1h in picro-Sirius red solution. After two washes in acidified water (5mL acetic acid glacial in 1L of water), the sections were dehydrated in three changes of 100% ethanol, cleared in xylene and mounted with a resinous medium. Stained liver sections were examined under a Leica DM5000 microscope. The METAVIR scoring system was used to determine the severity of hepatic fibrosis and the necro-inflammatory stage as previously described [97]. All samples were evaluated by the same pathologist, who was unaware of the laboratory data.

For immunofluorescence, 5 µm-thick sections were rehydrated by standard techniques and permeabilized with PBS, 0.5% Triton. Heat induced epitope retrieval using citrate buffer method (pH 6.0) were performed to unmask the antigen sites. The sections were then covered for 30 min with 75 mM NH_4Cl/PBS to reduce quenching and incubated for 1 hour at room temperature with blocking solution [3% bovine serum albumin (BSA; Sigma), 5% donkey serum (Millipore), 20 mM $MgCl_2$, 0.3% Triton in PBS pH 7.4]. Then, the sections were incubated over night at 4° C with the primary antibodies. The day after, sections were washed in PBS and then incubated with the secondary antibodies. Nuclei were counterstained with DAPI (Invitrogen). The secondary antibodies made in donkey were: AlexaFluor-594 anti-mouse (Invitrogen) and AlexaFluor-488 anti-rabbit (Invitrogen). Finally, the stained liver sections were mounted in mowiol, cover-slipped and examined under a Zeiss LSM 700 confocal laser-scanning microscope. The primary antibodies used for the immunofluorescence are listed in the **table 1**.

Immunofluorescence staining of apoptotic cells was performed by terminal deoxynucleotidyl transferase-mediated deoxyuridine triphosphate nick-end labeling

(TUNEL) using In Situ Cell Death Detection Kit (Roche Molecular Biochemicals) according to the manufacturer's instructions. Mice injected with 0.5 μg/g of body weight of CD95-activating antibody for 6 hours were used as positive control. The image capture was performed using Zeiss LSM 700 confocal laser-scanning microscope. The mean area and number of the ATZ globules by liver PAS-D staining were quantified using the ImageJ plug-in "Analyze particles" on the segmented images. Five different fields of view selected randomly for n=3 PiZ and PiZ/*Chop*$^{-/-}$ mice were used for the quantification. The image capture was performed using Leica DM5000 microscope.

For immunohistochemistry (IHC), 5 μm-thick sections were rehydrated and permeabilized in PBS/0.5% Triton (Sigma) for 20 minutes. Antigen unmasking was performed in 0.01 M citrate buffer in a microwave oven. Next, sections underwent blocking of endogenous peroxidase activity in methanol/1.5% H_2O_2 (Sigma) for 30 min and were incubated with blocking solution [3% BSA (Sigma), 5% donkey serum (Millipore), 1.5% horse serum (Vector Laboratories) 20 mM $MgCl_2$, 0.3% Triton (Sigma) in PBS] for 1 hour. Sections were incubated with primary antibody (**table 1**) overnight at 4°C and with universal biotinylated horse anti-mouse/rabbit immunoglobulin G secondary antibody (Vector Laboratories) for 1 hour. Biotin/avidin-horseradish peroxidase signal amplification was achieved using the ABC Elite Kit (Vector Laboratories) according to the manufacturer's instructions. 3,30-Diaminobenzidine (Vector Laboratories) was used as peroxidase substrate. Mayer's hematoxylin (Bio-Optica) was used for counterstaining. Sections were dehydrated and mounted in Vectashield (Vector Laboratories). Image capture was performed using the Leica DM5000 microscope.

3.3 Enzyme-linked immunosorbent assay (ELISA)

Liver protein extracts and serum samples were analyzed by enzyme-linked immunosorbent assay (ELISA) for ATZ detection. Multi-well plates (Nunc Maxisorp) were coated with cappel goat anti-human AAT (MP Biomedicals), and then blocked in

0.1% PBS Tween 20 containing 5% non-fat milk. Serial dilutions of purified human AAT (Athens Research and Technology) were loaded to build a standard curve. Rabbit anti-human AAT (Dako; 1:4000) was used as capturing antibody and goat anti-rabbit IgG-HRP (Dako; 1:2000) as secondary antibody. Then, 100 µL of chromogen substrate o-Phenylenediamine dihydrochloride (OPD; Sigma) was added to each well and incubated for 10 minutes in the dark. The reaction was stopped by adding 50 µL of 3 M H_2SO_4 to each well. The absorbance was measured at 450 nm using the PROMEGA GloMax Discover plate reader. In general, for the detection of the ATZ in the liver extracts and serum from PiZ mice were used 100 ng of total liver proteins, while the serum was diluted 1:216 000.

3.4 Real time PCR

Total RNA was extracted using RNeasy kit (Qiagen) and 1 µg of RNA was reverse transcribed using High-Capacity cDNA Reverse Transcription Kit (Applied Biosystems). PCR reactions were performed using SYBR Green Master Mix (Roche). PCR conditions were as follows: pre-heating, 5 min at 95°C; cycling, 40 cycles of 15 sec at 95°C, 15 sec at 60°C and 25 sec at 72°C. Results were expressed in terms of cycle threshold (Ct). Ct values were averaged for each duplicate. *β2-microglobulin (B2m)* was used as endogenous controls. Data were analyzed using LightCycler 480 software, version 1.5 (Roche). Primer sequences are listed in **table 2**.

3.5 Western blotting

Liver samples homogenized in RIPA buffer with protease and phosphatases inhibitors cocktail (Roche) were incubated for 20 min at 4°C and then centrifuged at 13,200 rpm for 10 min. The pellet was discarded and the supernatant was collected. Protein concentrations were measured using Coomassie Plus Bradford assay reagent (Thermo Scientific). Samples were denatured and reduced in Laemmli sample buffer containing

DTT for 5 min at 100°C and separated by SDS-PAGE. After transfer to PVDF membrane, blots were blocked in TBS-Tween20 containing 5% non-fat milk for 1 hour at room temperature followed by incubation with the primary antibody overnight at 4°C. Anti-rabbit IgG or anti-mouse IgG conjugated with horseradish peroxidase (HRP, GE Healthcare, 1:3,000) and ECL (Pierce) were used for detection. Primary antibodies used for immunoblots are listed in **table 1**. For the evaluation of protein localization, nuclear and cytoplasmic protein extracts were prepared using NXTRACT kit (Sigma-Aldrich) according manufacturer's instructions. In the western blot images, showed in the results section, each lane corresponds to an independent mouse.

3.6 Array expression analyses

Gene expression analysis was performed on 6-week-old male PiZ and C57/BL6 wild type mice (n=3 per group). All samples were processed on Affymetrix Mouse 430A 2.0 arrays using GeneChip 3'-IVT Plus and Hybridization Wash and Stain kits by means of Affymetrix's standard protocols. Raw intensity values of the 6 arrays were processed and normalized by Robust Multi-Array Average Method [98] using the Bioconductor [99] R package Affy [100]. Differentially expressed genes between conditions (PiZ vs. control) were identified using a Bayesian T-test [101]. For each p-value, the Benjamini-Hochberg procedure was used to calculate the False Discovery Rate (FDR) to avoid the problem of multiple testing. The selected gene lists were obtained using the following thresholds: false discovery rate (FDR) <0.05 and abs (ratio) >1.5. Data were deposited in GEO with the accession number GSE93115.

3.7 Gene Set Enrichment Analysis

Gene Set Enrichment Analysis (GSEA) [102] was performed using the GSEA software (www.broadinstitute.org/gsea). The list of differentially expressed genes between PiZ and wild type mouse livers was obtained by expression array profiling described above

(GSE93115). The set of CHOP target genes set was defined by combining ChIP-seq and RNA-seq data previously reported from tunicamycin-treated wild type mouse embryonic fibroblasts [103].

3.8 Protein co-immunoprecipitation

HeLa cells were co-transfected with the plasmid expressing CHOP-FLAG and plasmids expressing C/EBPβ or c-JUN. Untreated cells and cells co-transfected with the plasmid expressing CHOP-FLAG and a plasmid expressing GFP were used as controls. 48 hours after transfection, cells were washed with PBS and then, protein crosslinking was performed using a solution of 1.5 mM dithiobis (succinimidylpropionate) (DSP) (Thermo Fisher Scientific) in PBS added to the dishes. The dishes were incubated with DSP for 2 hours at 4°C. The reaction was stopped with the addition for 15 min at room temperature of 1 M Tris, pH 7.8, to a final concentration of 20 mM. The dishes were washed with PBS and then lysed as described above. 1 mg of protein lysates was used for the immunoprecipitation with mouse anti-FLAG antibody or mouse IgG over night at 4°C. The day after, 20 µL of Dynabeads Protein G (Thermo Fisher Scientific) were added to the tubes and incubated for 2 hours at 4°C. The flow-through was collected using the magnet and the complex Dynabeads-Ab-Ag was washed 5 times using RIPA buffer with 0.1% Triton without SDS and 1 time with RIPA buffer without Triton and SDS. Finally, the elution was performed by boiling tubes at 100°C for 5 minutes in a solution containing SDS 8%. Samples were analyzed by SDS-PAGE as described above. Primary antibodies used for immunoprecipitations are listed in **table 1**.

3.9 Luciferase assays

For generation of the plasmid with the *luciferase* gene, human *SERPINA1* regulatory regions were amplified by PCR from genomic DNA of PiZ mice. PCR product was cloned into a pGL3-Basic vector (Promega) upstream of the *firefly luciferase* (pAAT-

Luc vector). Since *SERPINA1* gene has also regulatory regions in the 3'untraslated region (UTR), the AAT 3'UTR was cloned downstream the *firefly luciferase* coding region in the pAAT-Luc vector (pAAT-Luc-AAT-3'UTR vector). The cDNA of human *c-JUN*, *CHOP*, and *c-FOS* were amplified by RT-PCR from HuH7 cells and cloned into p3xFLAG-CMV-14 vector. The plasmid expressing human *C/EBP*β was purchased from Origene (SC319561). AP-1 and CHOP-C/EBPβ heterodimers consensus sequences were mutagenized by QuickChange site-directed mutagenesis (Agilent). Primers used for generation of the constructs are shown in **table 3**. HeLa cells were cultured in DMEM in 10% fetal bovine serum (FBS) and 5% penicillin/streptomycin. Cells were co-transfected with the plasmid containing the wild type or mutagenized CHOP-C/EBPβ and AP-1 consensus sequences and with a plasmid expressing the human CHOP, C/EBPβ, and c-JUN. Each well was co-transfected with the pRL-TK plasmid (Promega) expressing the *renilla luciferase* as control. Lipo D293 (SigmaGen Laboratories) was used for the DNA transfection according to the manufacturer's instructions. Cells were harvested 48 hours after transfection and assayed for luciferase activity using the Dual-Luciferase Reporter (DLR™) Assay System (Promega). Data were expressed relative to renilla luciferase activity to normalize for transfection efficiency. Transfections were repeated at least three times.

3.10 Chromatin immunoprecipitations (ChIP)

PiZ mouse livers were mechanically homogenized in PBS in the presence of protein inhibitors and then crosslinked by formaldehyde to a final concentration of 1% for 10 minutes at room temperature. The cross-linking reaction was stopped by the addition of glycine at a final concentration of 0.125 mM for 5 minutes at room temperature. After three washes in PBS with protein inhibitors, liver homogenates were lysed in cell lysis buffer (piperazine-1,4-bis-2-ethanesulfonic acid 5 mM [pH 8.0], Igepal 0.5%, KCl 85 mM) for 15 minutes. Nuclei were lysed in lysis buffer (Tris HCl [pH 8.0] 50 mM, ethylene

diamine tetra-acetic acid 10 mM, SDS 0.8%) for 30 minutes. Chromatin was sonicated to yield DNA fragments approximately 200-1,000 bp. DNA was co-immunoprecipitated using the ChIP-grade anti-phospho-c-JUN (Ser73), anti-CHOP, and anti-C/EBPβ antibodies overnight at 4°C. No antibody was used in the negative control of the immunoprecipitation. Purified immunoprecipitated DNA samples and inputs were amplified by quantitative PCR with primers specific for the activator protein 1 (AP-1) and the C/EBPβ binding sites of the 5' untranslated region (5'-UTR) of the *SERPINA1* gene. *Gapdh* and *Rpl30* promoters were used as negative control regions whereas *p62*, *Gabarapl1*, and *Ctsl1* promoters were used as positive control regions with anti-CHOP and anti-C/EBPβ antibodies as previously showed [104, 105]. Antibodies for ChIP and primer sequences and are listed in **table 1 and 4**.

3.11 Human liver samples

Human liver samples were obtained from the Institute of Pathology, University Hospital of Basel (Basel, Switzerland) and St. Louis University School of Medicine, (St. Louis, MO, USA). Clinical and pathology features of these samples are shown in **tables 5** The Ethics Committees at each institution approved the study. Human liver samples used in **Fig. 3** and **10** were collected and anonymized according to applicable human studies approvals from subjects homozygous for the p.Glu342Lys mutation in *SERPINA1* gene and age-matched control subjects homozygous for the wild type allele of *SERPINA1* gene. PAS-D staining, immunohistochemistry and real-time PCR were performed as for mouse studies. *B2M* and *HPRT1* were used as housekeeping.

3.12 Statistical analyses

Data are expressed as averages ± standard deviation. Two tailed Student t test and analysis of variance (ANOVA) plus Tukey's post hoc analysis were used as statistical tests for mean comparisons. A p-value<0.05 was considered statistically significant.

Table 1: Primary antibodies and dilutions used.

Antibody	Manufacturer	WB dilution	IHC dilution	IF dilution	IP dilution	ELISA	ChIP
anti-CHOP	Abcam (ab11419)	1/500	1/100	-	-	-	-
anti-CHOP	LifeSpan Biosciences (LS-B3652)	-	1/40	-	-	-	-
anti-GAPDH	Santa Cruz Biotech (sc-365062)	1/3000	-	-	-	-	-
anti-LAMIN-A	Abcam (ab26300)	1/1000	-	-	-	-	-
anti-AAT	DAKO (A0012)	-	-	-	-	1/4000	-
anti-ATZ polymer	Hycult Biotech (HM2289)	-	-	1/100	-	-	-
anti-FLAG	Sigma (F1804)	-	-	-	1/200 (3µg)	-	-
anti-FLAG	Sigma (F7425)	1/2000	-	-	-	-	-
anti-C/EBPβ	Abcam (ab220813)	1/1000	-	-	-	-	-
anti-CALNEXIN	Enzo Life Sciences (ADI-SPA-860)	1/1000	-	-	-	-	-
IgG mouse	Santa Cruz Biotech (sc-2025)	-	-	-	1/80 (3µg)	-	-
Anti-CHOP	Cell signaling (2895)	-	-	-	-	-	1/100
Anti-C/EBPβ	Abcam (Ab15050)	-	-	-	-	-	1/200
Anti-Myc	Cell signalling (2278)	1/1000	-	-	-	-	-
Anti-phospho-c-JUN	Cell signalling (3270)	1/500	-	-	-	-	1/100
Anti-c-JUN	Cell signalling (9165)	1/500	-	-	-	-	-
Anti-phospho-JNK1/2	Cell signalling (4668)	1/500	-	-	-	-	-
Anti-JNK1/2	Cell signalling (9252)	1/500	-	-	-	-	-
Anti-Histone H3	Cell signalling (4499)	1/3000	-	-	-	-	-

Table 2: Sequence of primers used for qPCR

Gene	Forward (5'-3')	Reverse (5'-3')
mChop	CACCACACCTGAAAGCAGAA	TCCTCATACCAGGCTTCCAG
mβ2m	TGGTGCTTGTCTCACTGACC	GTATGTTCGGCTTCCCATTC
hSERPINA1	TGCCCAGGTATTTCATCAGC	CCGTGAAGGTGCCTATGATG
hCHOP	GGAAACAGAGTGGTCATTCCC	CTGCTTGAGCCGTTCATTCTC
hSQSTM1	CAAGTGACATGAAGGGAGGGT	ATGTGCTGGGCTGCTAACGTAG
hATF3	GCTGGAAAGTGTGAATGCTG	CTGAGCCCGGACAATACAC
hTRIB3	GCCTTTTTCACTCGGACCCAT	CAGCGAAGACAAAGCGACAC
hSLC20A1	AGCGTGGACTTGAAAGAGGA	TCTTTGTACAGGCCGGAATC
hALH18A1	GCACACAGCAACCGGATT	AGAGCCACGTGGAATGATCA
hCYB5R1A	CATCAGGCCATACACTCCTG	GCTATCCAGGTACTGAGACATC
hMTM1	GCCTTACGCGACGAATACAT	GTGAAGTTGGGGGATCAGAAAG
hLGALS3	CAATTCTGGGCACGGTGAA	TGAAGCGTGGGTTAAAGTGG
hGTPBP2	GAAGGCAGTGGTACGTTTCC	GCTTCTCCTGCTGTAATGGC
hUBE2G2	GAGAAGATCCTGCTGTCGGT	TAGAACTGCTCCCGGTCATC
hHPRT1	CCTGGCGTCGTGATTAGTGAT	AGACGTTCAGTCCTGTCCATAA

Table 3: Primers for generation of plasmids used in the luciferase assay and in immunoprecipitation studies.

Gene	Forward (5'-3')
pAAT-LUC-FW	CGGggtaccTGCACTCATCCATTCACTCTGC
pAAT-LUC-REV	CCCaagcttTCTCCAGAACCTCTCGCAGT
3'UTR-AAT-FW	GCtctagaCTGCCTCTCGCTCCTCAAC
3'UTR-AAT-REV	GCtctagaTGCAAGAAATGTAGTTCTATTTATTCTCTG
c-JUN-FW	ATTTgcggccgcATGACTGCAAAGATGGAAACG
c-JUN-REV	CCGgaattcAAATGTTTGCAACTGCTGCG
AP-1 site1mut-FW	CTGGTAGCAAGATCTACCATTTACCAAGCAACCCCAAAATGC CTGATGCTGAAG
AP-1 site1mut-REV	CTTCAGCATCAGGCATTTTGGGGTTGCTTGGTAAATGGTAGA TCTTGCTACCAG
AP-1 site2mut-FW	GAGGGGGTGGCGCAAGCAAGACAGTCTCTGGGAGAGTACCA
AP-1 site2mut-REV	TGGTACTCTCCCAGAGACTGTCTTGCTTGCGCCACCCCCTC
CHOP-FW	ATAAGAATgcggccgcATGGAGCTTGTTCCAGCCA
CHOP-REV	CCGgaattcccTGCTTGGTGCAGATTCACC
c-FOS-FW	ATAAGAATgcggccgcATGATGTTCTCGGGCTTC
c-FOS-REV	CCGgaattcccCAGGGCCAGCAGCGTGGGTG
c-JUN-Myc-FW	CCCaagcttATGACTGCAAAGATGGAAACG
c-JUN-Myc-REV	CCGgaattcCCAAATGTTTGCAACTGCTGCG
CHOP-C/EBPβ site1mut- FW	CCTTTAAAAGCCTAAATCAGAGGAGATCGCCCGCTGTGCAAC CCGCA
CHOP-C/EBPβ site1mut- REV	TGCGGGTTGCACAGCGGGCGATCTCCTCTGATTTAGGCTTTT AAAGG
CHOP-C/EBPβ site2mut- FW	GTGGGGCCCCACTTGAGGAGAATCCCTTTAAAAGCCTAAATC AGATTGCAT
CHOP-C/EBPβ site2mut- REV	ATGCAATCTGATTTAGGCTTTTAAAGGGATTCTCCTCAAGTG GGGCCCCAC

Small case letters indicate nucleotides used to add restriction enzyme digestion sites. AP-1 site1mut, AP-1 site2mut, CHOP-C/EBPβ site1mut, and CHOP-C/EBPβ site2mut are the primers used for site-directed mutagenesis showed in **Fig. 21**; mutagenized nucleotides are underlined.

Table 4: qPCR primers used for the chromatin immunoprecipitation (ChIP) experiments.

Gene	Forward (5'-3')	Reverse (5'-3')
AP-1 sites	CGGCAGTAAGTCTTCAGCATC	CTGCACTTACCGAAAGGAGTC
CHOP-C/EBPβ sites	TATCTACGGCACGTACGCCA	AGGTACAGGGTTGAGGCTAGTG
p62/Sqstm1	CCTGGTTTTGGCGTTTGTAT	GGGATACAGGTCATGAGGATTT
Gabarapl1	GGCACTTTTCCAACTCCAGA	TCCCTCCCCTTCAAGTTTCT
Ctsl1	AAAATGTGCAGGGTGGAGAG	TGTCCTCCGCTCTGTCTTCT
Gapdh	GCCTCAGATCGCTGCTCT	GGAGGAAAAGGATGAGATGAG
Rpl30	CCCTCCATTACCTCAAAGCTG	GTACGTGCTGGGCTACAAGC

Table 5: Clinical and pathology features of alpha1-antitrypsin deficiency patients and controls.

Reference	Gender	Age (years)	Diagnosis
Control #1	M	41	Focular nodular hyperplasia
Control #2	F	46	Focular nodular hyperplasia
Control #3	F	71	Focular nodular hyperplasia
PiZZ #1	M	90	Chronic hepatitis
PiZZ #2	M	66	Chronic hepatitis
PiZZ #3	M	70	Chronic sclerosis steatohepatitis, eosinophil infiltration

Chapter 4: Results

To investigate the molecular mechanism underlying the pathogenesis of the disease, I used the PiZ mouse model, a transgenic mouse genetically engineered to express the Z allele of human *SERPINA1* gene under the control of its promoter region. This model has been a valuable model for studying the liver disease induced by ATZ and for the development of novel therapies. In PiZ mouse livers, ATZ accumulates within the ER of hepatocytes as periodic acid Schiff-diastase resistant (PAS-D) positive globules in a nearly identical manner to livers of human patients [92]. In addition, in these mice the accumulation of ATZ induces liver injury resulting in an inflammatory response, fibrosis and increased frequency of HCC [106, 107]. However, because the murine genes for the AAT are not mutated, these mice showed normal levels of circulating murine AAT proteins and they do not present the lung phenotype.

Mice have multiple genes encoding AAT and a mouse model deleted for all *Serpina1* paralogs has been recently generated by using CRISPR/Cas9 genome editing [108]. These mice recapitulate the features of human lung disease related to AATD, including absence of circulating AAT, reduced capacity to inhibit neutrophil elastase, and emphysema. However, as expected this mouse model does not develop a liver disease that is due a gain of function mechanism, caused by accumulation of mutant *SERPINA1* variants in the liver.

Section 1: JNK signaling and AATD

In this section, I will first provide an overview of the roles of c-JUN N-terminal kinase (JNK) in physiology and disease states and next I will describe the results we recently obtained about the role of JNK in the pathogenesis of liver disease associated to AATD. These data have been published in 2017 in the journal "*Hepatology"* [109].

4.1 c-JUN N-terminal kinase (JNK) signaling pathway

The mitogen-activated protein kinase (MAPK) pathway is an important regulatory mechanism, conserved in all eukaryotic cells. The three best characterized subfamilies of MAPK proteins are named extracellular signal-regulated kinase (ERK), c-JUN N-terminal kinase (JNK), and p38. There are three genes that encode JNK protein kinases in mammals: *Jnk1*, *Jnk2* and *Jnk3*. Among these, *Jnk1* and *Jnk2* are ubiquitously expressed, whereas *Jnk3* expression is restricted to the brain, testis and heart [110, 111]. These genes are alternatively spliced to create ten isoforms [112]. Transcripts derived from all three genes encode protein with and without a C-terminal extention, generating both 46kDa and 55kDa isoforms. The functional significance of this isoforms is still poorly understood.

JNK protein kinases are activated by different stress stimuli, including UV irradiation and osmotic or oxidative stress. After activation by upstream kinases, they regulate various physiological processes in cells, including inflammation, stress, cell growth, cell development, differentiation and death [113].

The activating protein 1 (AP-1) family of transcription factors is among the best characterized targets of JNKs. AP-1 family includes structurally and functionally related members of the JUN (c-JUN, JUNB and JUND), FOS (c-FOS, FOSB, FRA-1 and FRA-2), and ATF (ATF2, ATF3 and ATF7) families. Additionally, new proteins have recently been added to the AP-1 family such as MAF proteins (v-MAF and c-MAF) and JUN-dimerizing proteins (JDP1 and JDP2) [114, 115].

A common feature of all these proteins is the evolutionarily conserved bZIP domain, composed by a basic DNA-binding domain and leucine zipper domain, responsible for dimerization. Like all bZIP transcription factor, AP-1 proteins have to dimerize before they can bind to their DNA target sequences. JUN proteins form stable homo- and heterodimers, whereas FOS proteins cannot form homodimers. JUN homodimers and JUN-FOS heterodimers preferentially bind to the phorbol 12-O-tetradecanoate-13-acetate (TPA)-responsive element (TRE, consensus sequence:

TGACTCA). On the other hand, JUN-ATF heterodimers and ATF homodimers preferrentially bind the cAMP-responsive element (CRE, consensus TGACGTCA) [116]. Both elements are palindromic and contain the same AP-1 half site.

JNK proteins are known to phosphorylate c-JUN on two serine residues (amino acid positions 63 and 73), leading to its nuclear translocation. JNK-dependent phosphorylation of c-JUN increases also its transcriptional activity and stability [117, 118]. JNK/c-JUN signaling pathway has been implicated in different biological processes, including autophagy, cell differentiation and survival, apoptosis and tumor development [113, 114]. In light of its implication in different disease, different drugs targeting JNK/c-JUN signaling have been developed. One of this is a small molecule named SP600125, which inhibits all 3 JNK proteins by competing with the ATP-binding site and results also in reduced c-JUN phosphorylation [119].

4.2 The JNK pathway is activated in mouse and human livers expressing ATZ

To investigate the pathogenesis of liver damage induced by ATZ, we analyzed livers of 6-week-old PiZ mice and wild type controls by expression array profiling. Analysis of "biological functions" terms indicated that most genes up-regulated in PiZ livers were associated with response to unfolded proteins, response to ER stress, ER nuclear signaling pathway, and response to protein stimulus (**Fig. 1A**). Search Tool for the Retrieval of Interacting Genes (STRING) analysis that takes into consideration gene-gene and protein-protein interactions revealed enrichment of genes induced by cellular response to stress, including JNK and c-JUN (**Fig. 1B)** which have not previously found to be affected in livers expressing ATZ.

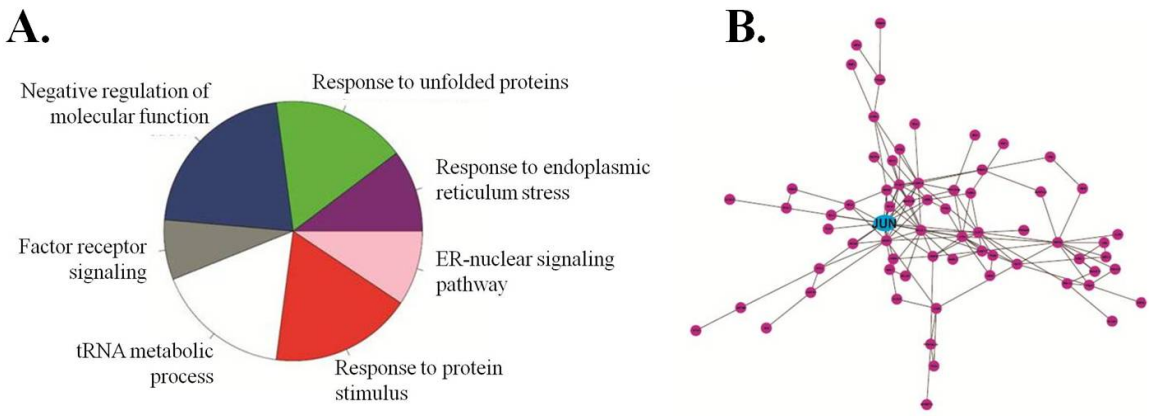

Figure 1: Expression RNA profiling and protein-protein interactions in PiZ mouse livers.
(**A**) Genes up-regulated in PiZ mice were associated with the response to unfolded proteins, response to ER, ER nuclear signaling pathway, and response to protein stimulus. Livers of 6-week-old PiZ mice (n=3) and age-matched and gender-matched controls (n=3) were used for expression array profiling. (**B**) Search Tool for the Retrieval of Interacting Genes analysis showed enrichment on genes of cellular response to stress including c-JUN.

We confirmed c-JUN activation by the increased levels of phospho-c-JUN in PiZ mouse livers compared to wild type controls **(Fig. 2A).** C-JUN is one of the main cellular substrate activated by JNK through phosphorylation [120] and indeed a significant increase of phosphorylated JNK was observed in PiZ mouse livers (**Fig. 2B**). To investigate the role of JNK *in vivo*, we crossed PiZ mice with *Jnk1* or *Jnk2* knock-out mice [93, 94]. Being c-JUN a target of JNK, as expected PiZ/*Jnk1*$^{-/-}$ and PiZ/*Jnk2*$^{-/-}$ mice showed reduced hepatic phospho-c-JUN/total c-JUN compared to PiZ mice (**Fig. 2A, C**). Upon phosphorylation c-JUN translocates to the nucleus where activates its target genes. Consistently with c-JUN phosphorylation, we also found increased levels of phospho-c-JUN in the nuclear extracts of PiZ mouse livers compared to control wild type mice and compared to either PiZ/*Jnk1*$^{-/-}$ or PiZ/*Jnk2*$^{-/-}$ mouse livers (**Fig. 2D**).

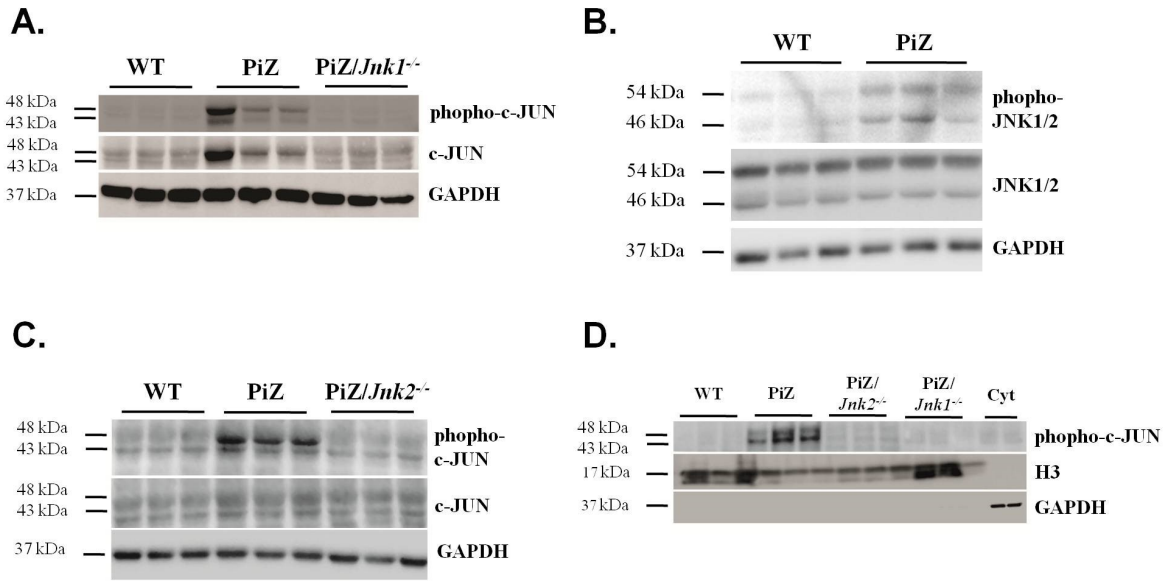

Figure 2: Activation of the JNK signaling in PiZ mouse livers.
(**A**) Western blotting of phosphorylated and total c-JUN in 6-week-old PiZ mouse livers compared to wild type (WT) controls and PiZ/*Jnk1*$^{-/-}$. (**B**) Western blotting of phosphorylated and total JNK in 6-week-old PiZ mouse livers compared to WT controls. (**C**) Western blotting of phosphorylated and total c-JUN in 6-week old PiZ mouse livers compared to WT controls and PiZ/*Jnk2*$^{-/-}$. (**D**) Western blotting of phosphorylated c-JUN on nuclear extracts of livers of WT, PiZ, PiZ/*Jnk2*$^{-/-}$, and PiZ/*Jnk1*$^{-/-}$ mouse livers. Nuclear extracts were positive for the histone H3 but negative for the cytosolic GAPDH protein. The cytosolic fraction was negative for H3 and positive for GAPDH. Abbreviations: GAPDH, glyceraldehyde 3-phosphate dehydrogenase; phospho, phosphorylated.

To interrogate the clinical relevance of our findings, we determined whether JNK is also activated in human livers from PIZZ patients. Liver samples were obtained from five PIZZ patients under 18 years of age homozygous for the p.Glu342Lys mutation in *SERPINA1* who underwent hepatic transplantation for liver failure. Three control liver specimens were obtained from age-matched patients homozygous for the wild type allele of *SERPINA1* gene who also underwent liver transplantation. As expected, in addition to cirrhosis, livers of PIZZ patients showed accumulation of PAS-D positive globules that was not detected in control livers (**Fig. 3A**). Livers of PIZZ patients showed greater activation of JNK compared to controls, as shown by increased phosphorylated JNK (**Fig. 3B**), thus confirming the findings of activated JNK also in livers of patients with AATD.

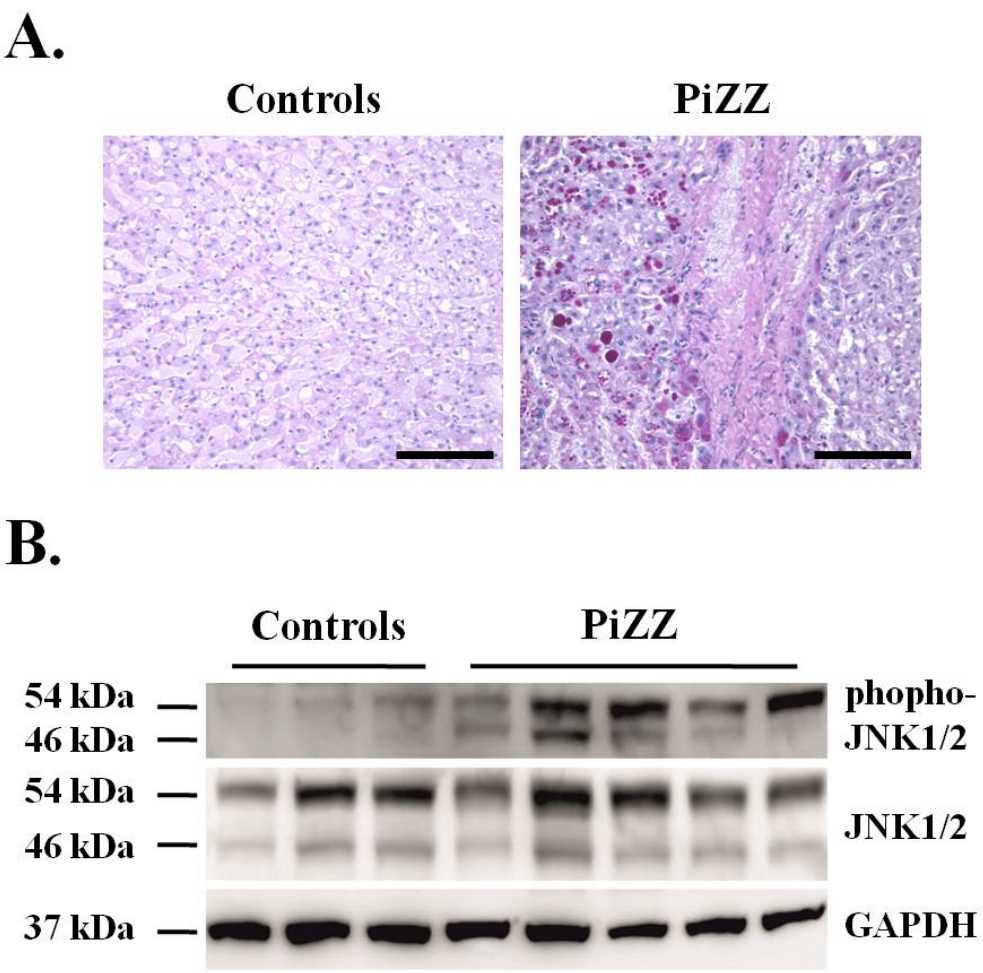

Figure 3: Activation of the JNK signaling in human livers from PiZZ patients.
(**A**) Representative PAS-D staining from a PIZZ patient with cirrhosis who underwent liver transplantation, and a control liver from a patient with liver failure due to an unrelated disease (20X magnification, scale bar 100µm). (**B**) Western blotting of phosphorylated and total JNK in livers of five PIZZ patients and three controls from patients with liver failure due to unrelated diseases. Abbreviation: phospho, phosphorylated.

Taken together these results showed activation of the JNK/c-JUN signaling in mouse and human livers expressing ATZ.

4.3 *Jnk1* and *Jnk2* deletion reduces ATZ accumulation in PiZ mouse livers

Compared to PiZ, livers of PiZ/*Jnk1*$^{-/-}$ mice showed reduced ATZ by PAS-D staining, immunofluorescence for the polymeric ATZ and ELISA on liver homogenates (**Fig. 4A, 4B, and 5A**).

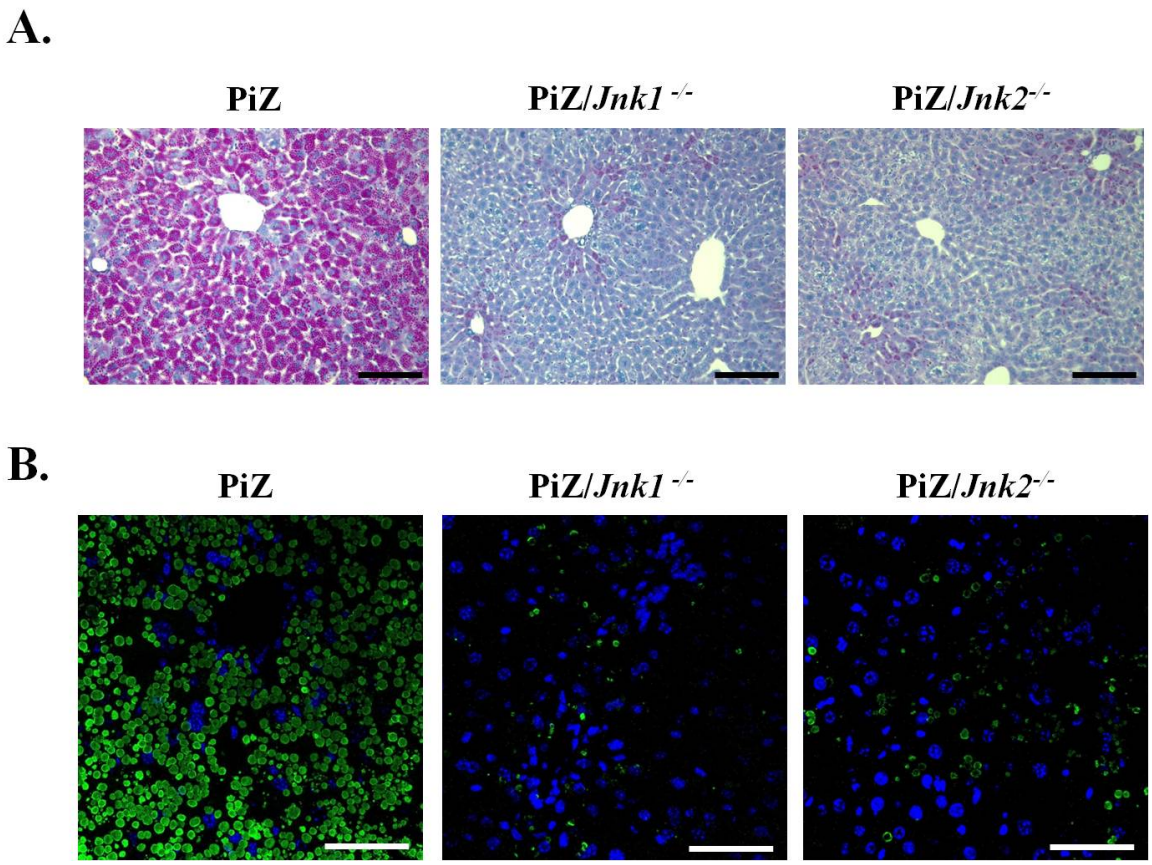

Figure 4: Deletion of *Jnk1* and *Jnk2* reduces hepatic ATZ accumulation in PiZ mouse livers.
(**A**, **B**) Representative PAS-D staining (upper panels, 20X magnification, scale bar 100µm) and immunofluorescence (lower panels, 63X magnification, scale bar 50µm) for the polymeric ATZ on livers of PiZ, PiZ/*Jnk1*$^{-/-}$, and PiZ/*Jnk2*$^{-/-}$ mice.

In addition, PiZ/*Jnk1*$^{-/-}$ mice showed also reduced serum ATZ levels compared to wild type control mice (**Fig. 5B**).

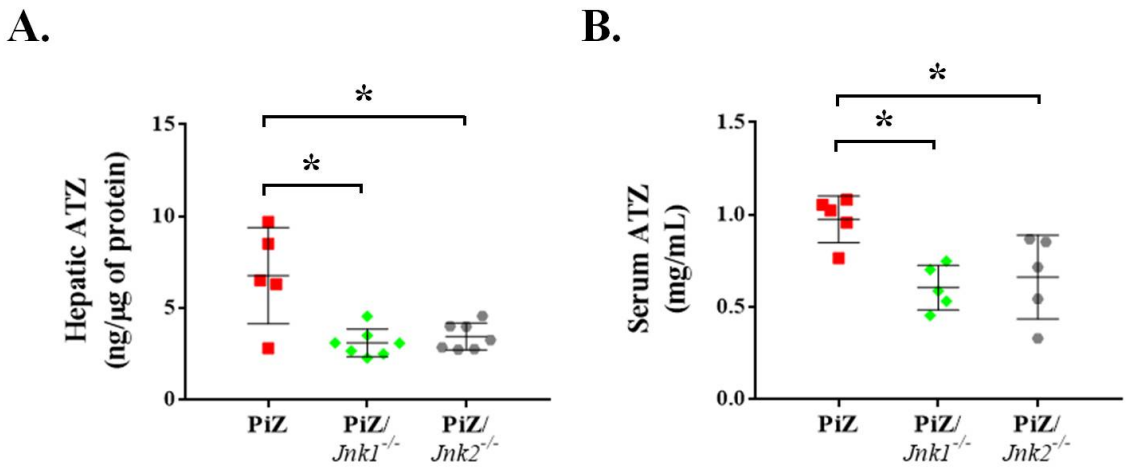

Figure 5: Deletion of *Jnk1* and *Jnk2* decreases hepatic and serum ATZ levels.
(**A**, **B**) ATZ ELISA on livers and serum of PiZ, PiZ/*Jnk1*$^{-/-}$ and PiZ/*Jnk2*$^{-/-}$ mice (at least n=5 per group) Averages ± standard deviations are shown. *t*-test: *p-value< 0.05.

SERPINA1 mRNA levels in livers of PiZ/*Jnk1*$^{-/-}$ mice were also significantly reduced compared to PiZ controls (**Fig. 6A**), suggesting that JNK induces ATZ accumulation by increasing *SERPINA1* transcription. Like PiZ/*Jnk1*$^{-/-}$ mice, PiZ/*Jnk2*$^{-/-}$ mice showed similar reductions of ATZ by PAS-D staining (**Fig. 4A**), immunofluorescence for the polymeric ATZ (**Fig. 4B**), ELISA on the liver extracts and serum (**Fig. 5A, B**), and real time PCR (**Fig. 6A**) compared to age-matched control wild type mice.

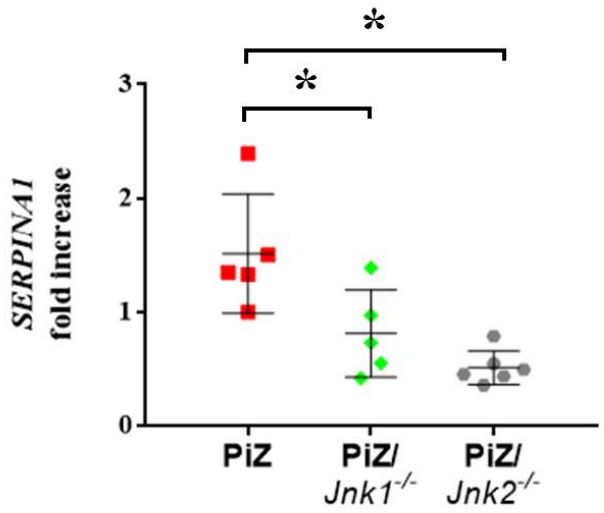

Figure 6: *SERPINA1* expression in PiZ, PiZ/*Jnk1*$^{-/-}$, and PiZ/*Jnk2*$^{-/-}$ mouse livers.
Real time PCR for the *SERPINA1* gene in PiZ, PiZ/*Jnk1*$^{-/-}$, and PiZ/*Jnk2*$^{-/-}$ mouse livers (at least n=5 per group). *β2-microglobulin* was used for normalization. Averages ± standard deviations are shown. *t*-test: *p-value< 0.05.

4.4 c-JUN regulates *SERPINA1* expression

SERPINA1 gene is transcriptionally regulated at least by two tissue-specific regulatory regions located in the 5'-UTR: the liver-specific regulatory region located upstream of the non-coding exon 1C and a second regulatory region upstream of exon 1A that controls expression in monocytes [28]. The liver-specific regulatory region at the 5'-UTR contains two putative binding sites for AP-1 [27] that is composed of c-FOS and c-JUN [27] (**Fig. 7A**). Therefore, we hypothesized that expression and accumulation of ATZ is dependent upon increased JNK-mediated activation of c-JUN and subsequent *SERPINA1* up-regulation. In support of this hypothesis, I found an enrichment of AP-1 binding sites in chromatin immunoprecipitates with anti-phosphorylated c-JUN antibody on PiZ mouse

livers (**Fig. 7B**). Moreover, to further investigate the *SERPINA1* regulation, I constructed a plasmid including the firefly luciferase gene under the control of the hepatic regulatory region at the 5'-UTR of the human *SERPINA1* gene including the two putative AP-1 binding sites (**Fig. 7A**). HeLa cells co-transfected with this plasmid and a plasmid expressing c-JUN showed increased levels of luciferase compared to cells co-transfected with the control plasmid (**Fig. 7C**). The luciferase activity was significantly reduced when the one or two binding sites for c-JUN were mutagenized (**Fig. 7C**). Taken together, these results show that c-JUN up-regulates *SERPINA1* expression through binding and transactivation of the AP-1 sites at the 5'UTR of the *SERPINA1*.

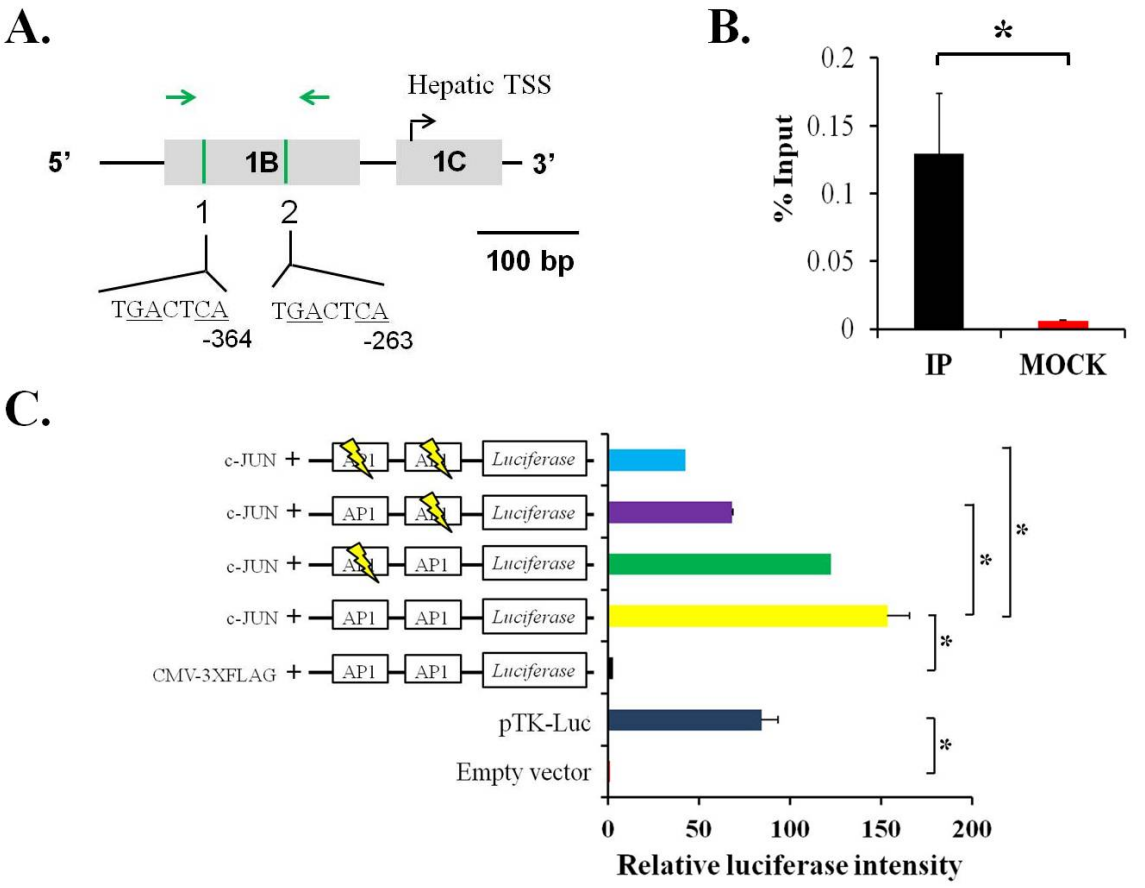

Figure 7: c-JUN regulates *SERPINA1* expression.
(**A**) Schematic representation of the two putative AP-1 binding sites (consensus sequence 5'-TGACTCA-3') in the 5'-UTR of the *SERPINA1* gene (drawn to scale). The hepatocyte regulatory region is located at positions –364 (site 1) and –263 (site 2) from the hepatic transcription starting site (TSS)(30) (genomic position site 1, chr14:94388968-94388974; site 2, chr14, 94388867-94388873, GRCh38/hg38 assembly). Green arrows show the position of the primers used for real-time PCR amplification of the ChIP shown in (**B**). ChIP with anti-phosphorylated c-JUN antibody on PiZ mouse livers showed enrichment of the 5'-UTR region containing the two AP-1 binding sites of the *SERPINA1* gene. The ChIP results were obtained by three independent experiments and are shown as percentage of input. (**C**) Luciferase activity in HeLa cells co-transfected with a plasmid containing the human *SERPINA1* enhancer regions with two AP-1 putative binding sites upstream of the *firefly luciferase* coding region and plasmid expressing the human c-JUN. Experiments were performed in duplicate. Mutagenized constructs co-transfected with c-JUN plasmid were compared to non-mutagenized construct co-transfected with c-JUN. Averages ± standard deviations are shown. *t*-test: *p-value< 0.05. Abbreviations: Cyt, cytosolic fraction; 1B, exon 1B; 1C, exon 1C; IP, immunoprecipitated DNA; TSS, transcription start site.

Section 2: the transcription factor CHOP and AATD

In this section, I will provide an overview about the function of CHOP and I will next describe the results about its role in the pathogenesis of liver disease associated to AATD. At the time of the thesis writing, these data presented in this section are being submitted to *Hepatology*.

4.5 The transcription factor CHOP

CHOP, also known as DNA damage inducible transcript 3 (DDIT3), is a transcription factor involved in the ER stress response. Its expression is induced by a variety of stress conditions including genotoxic stress, hypoxia, glucose and amino acid deprivation, ER stress and unfolded protein response (UPR) [121-125]. First described to be involved in ER-stress mediated apoptosis [126], CHOP was found to play a role in many other physiological functions such as lipid metabolism, energy metabolism and inflammatory response [127, 128]. It is a 29 kDa protein with 169 (human) and 168 (mouse) amino acid residues, composed by two functional domains: the N-terminal activation domain and the C-terminal basic-leucine zipper (bZIP) domain [129]. Under non stressed-condition, CHOP is ubiquitously expressed at very low levels and mainly located in cytoplasm whereas stress conditions lead to its up-regulation and translocation to the nucleus [130]. Its expression is regulated by several transcription factors, including ATF4, XBP-1, ATF6, Farnesoid X receptor (FXR), and c-JUN [131-135]. At the post-transcriptional level, CHOP was found to be phosphorylated on two close serine residues by the p38 MAPK [136]. CHOP is implicated in numerous human diseases, such as neurodegenerative disease, diabetes, ischemic diseases, tumor, and liver diseases [137-143]. CHOP is also a positive regulator of autophagy and drives the transcription of several autophagy-related genes (Atg), including *Atg5*, *Atg7* and *p62/Sqstm1* [104].

Considering its implications in different pathological conditions, drug that can inhibit CHOP signaling may be therapeutically beneficial. Although some small molecules

resulting in CHOP reduction have been developed [144], a specific and efficient drug is still lacking.

4.6 CHOP is activated in mouse livers expressing ATZ

In the expression array profiling on PiZ livers shown in **Fig. 1**, several up-regulated genes are related to response to ER stress [109]. Among differentially expressed genes, the transcription factor CHOP was among the most up-regulated. Compared to age-matched wild type controls, *Chop* showed a significant 12- and 1.9-fold up-regulation in 6- and 36-week-old PiZ mouse livers, respectively by real time PCR (**Fig. 8A**). To interrogate the clinical relevance of our findings, I also investigated CHOP levels and activation in two different sets of livers of PiZZ patients. Compared to controls taken from adult individuals with focal nodular hyperplasia, in liver biopsies of three adult PiZZ patients with chronic liver disease I detected a 3-fold up-regulation of *CHOP* mRNA levels (**Fig. 8B, Table 5**).

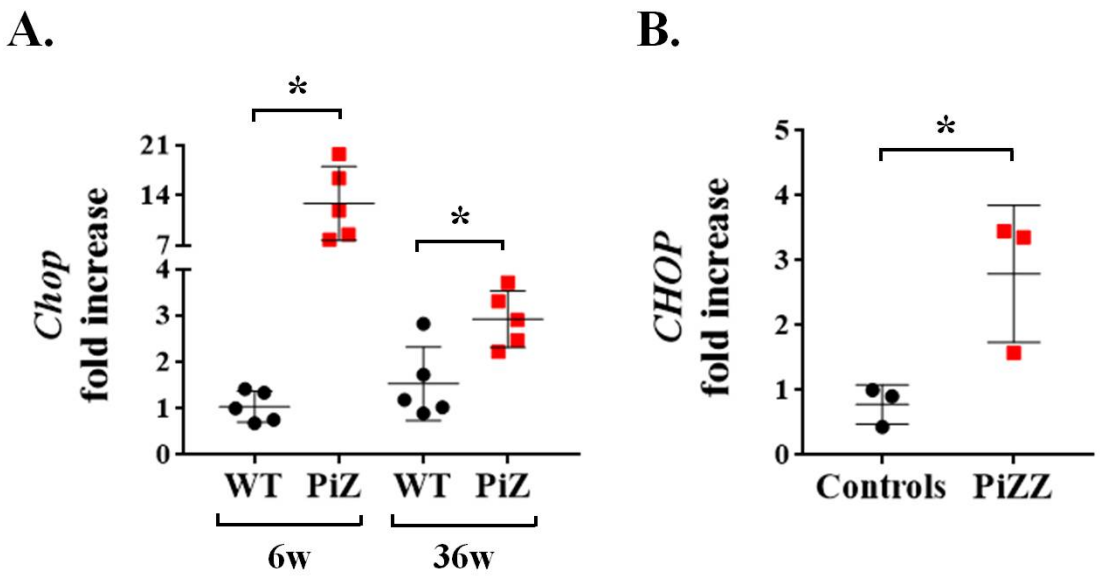

Figure 8: CHOP is up-regulated in mouse and human livers expressing ATZ.
(**A**) *Chop* expression in livers of wild type (WT) and PiZ mice of 6 and 36 weeks of age (n=5 per group). *β2-microglobulin* was used for normalization. (**B**) *CHOP* expression in liver biopsies from PiZZ patients and controls with focal nodular hyperplasia (n=3 per group). *β2M* and *HPRT1* were used for normalization. Averages ± standard deviations are shown. *t*-test: *p-value < 0.05. Abbreviations: 6W, 6-week-old; 36W, 36-week-old.

Increased expression of CHOP was confirmed at the protein level in 6- and 36-week-old PiZ mouse livers (**Fig. 9A**). Compared to wild type controls, PiZ mouse livers showed

increased CHOP levels by western blot also on nuclear extracts at 6-weeks of age, like mice injected with tunicamycin, an inducer of ER stress and CHOP expression (**Fig. 9B**).

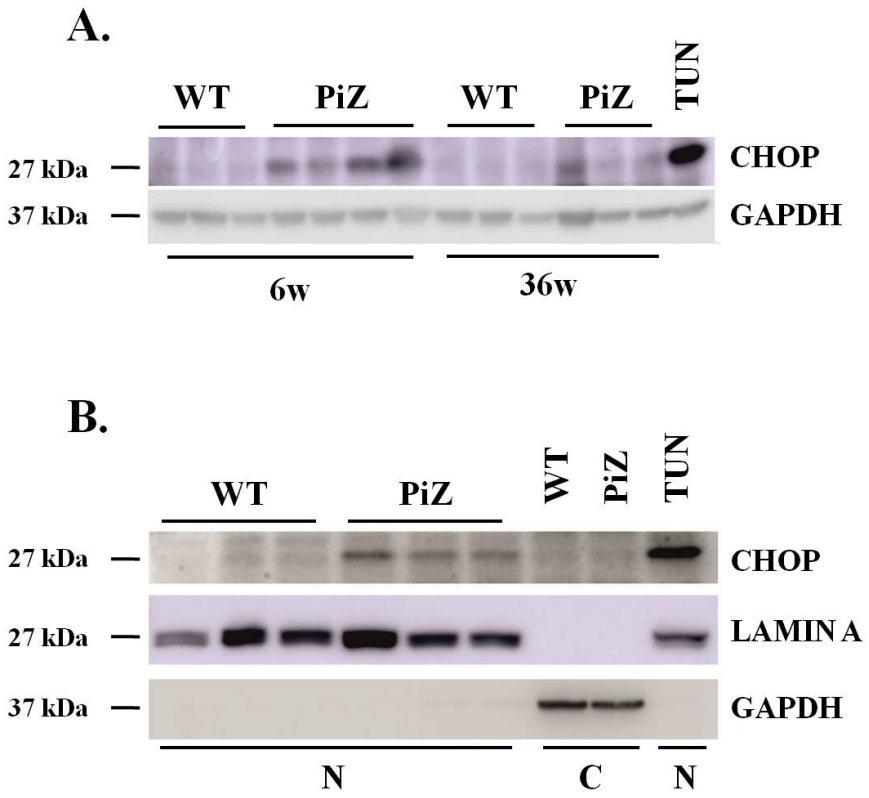

Figure 9: CHOP is activated in PiZ mouse livers.
(**A**) Western blotting of CHOP in livers of wild type (WT) and PiZ mice of 6 and 36 weeks of age. A liver of a WT mouse injected intra-peritoneally with 4 µg/g tunicamycin (TUN) was used as a positive control. (**B**) Western blotting of CHOP on nuclear extracts of 6-week-old WT and PiZ mouse livers. Lamin A was used as nuclear marker and GAPDH as cytosolic marker. Abbreviations: 6W, 6-week-old; 36W, 36-week-old; N, nuclear extracts; C, cytosolic extracts; TUN, tunicamycin.

Increased nuclear CHOP in PiZ livers was confirmed by immunohistochemistry (IHC) in 6- and 36-week old PiZ mouse livers (**Fig. 10A**). In a second set of liver samples from PiZZ adults patients with extensive PAS-D staining (**Fig. 10B**, upper panels**)** and end-stage liver disease requiring liver transplantation [109], increased CHOP nuclear signals was detected by IHC compared to controls (**Fig. 10B,** lower panels).

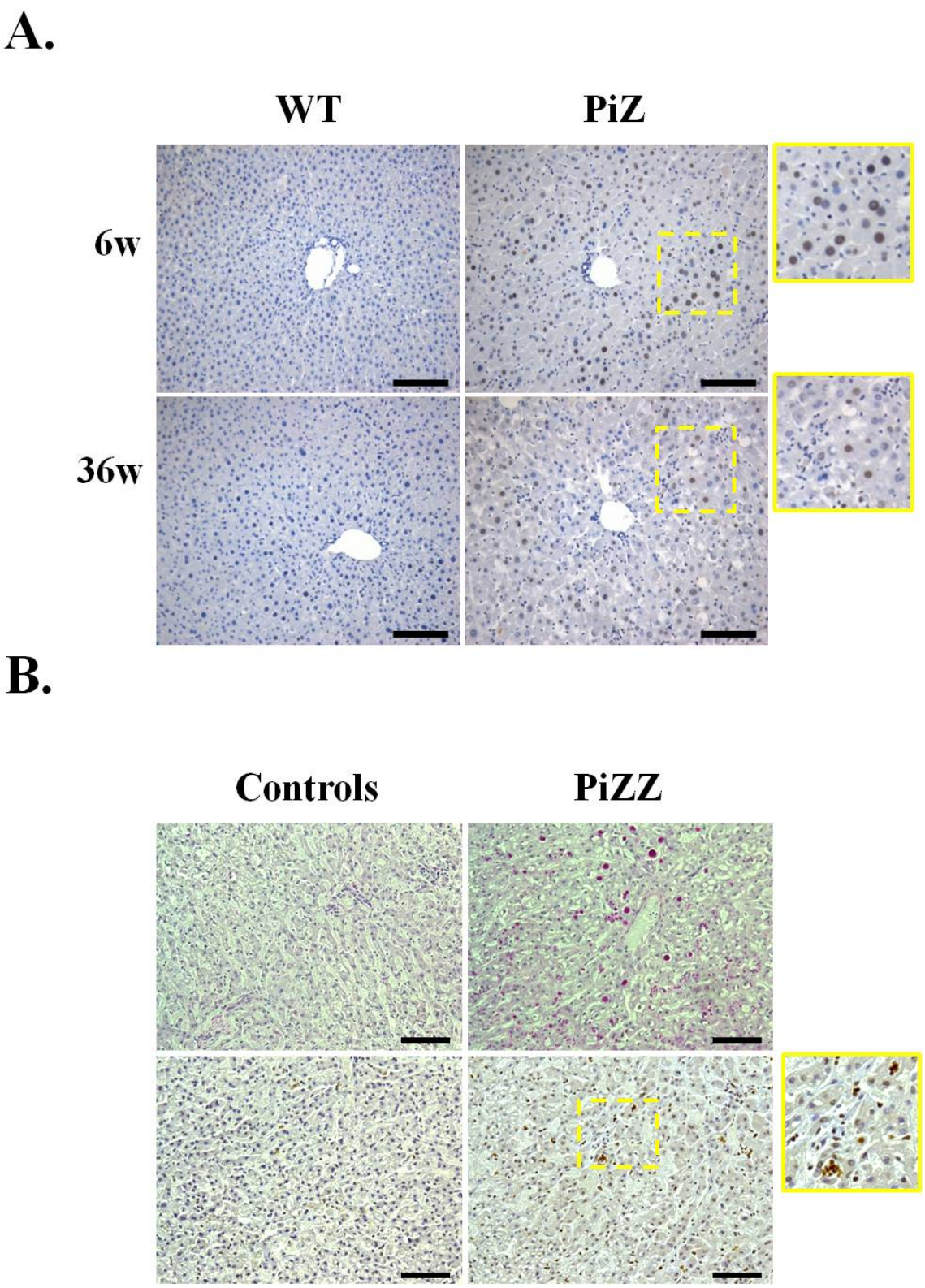

Figure 10: CHOP activation in mouse and human livers expressing ATZ.
(**A**) Representative immunohistochemistry (IHC) with anti-CHOP antibody in 6- and 36-week-old wild type (WT) and PiZ mouse livers (40X magnification, scale bar 50μm). (**B**) Representative PAS-D staining (upper panels) and IHC with anti-CHOP antibody (lower panels) in liver of PiZZ patients with end-stage liver disease underwent to liver transplantation and age-matched PiMM patients who also underwent to liver transplantation as controls (20X magnification, scale bar 100μm).

Gene Set Enrichment Analysis (GSEA) with microarray expression data (showed in **Fig. 1A**) showed also an enrichment of up-regulated CHOP target genes in PiZ livers compared to wild type controls (enrichment score [ES]=0.58) (**Fig. 11A**). Up-regulation of CHOP target genes, selected among the most up-regulated orthologues in PiZ mouse livers, was also confirmed by qPCR on human liver biopsies from adult PiZZ patients with chronic liver disease and adult controls (**Fig. 11B, Table 5**).

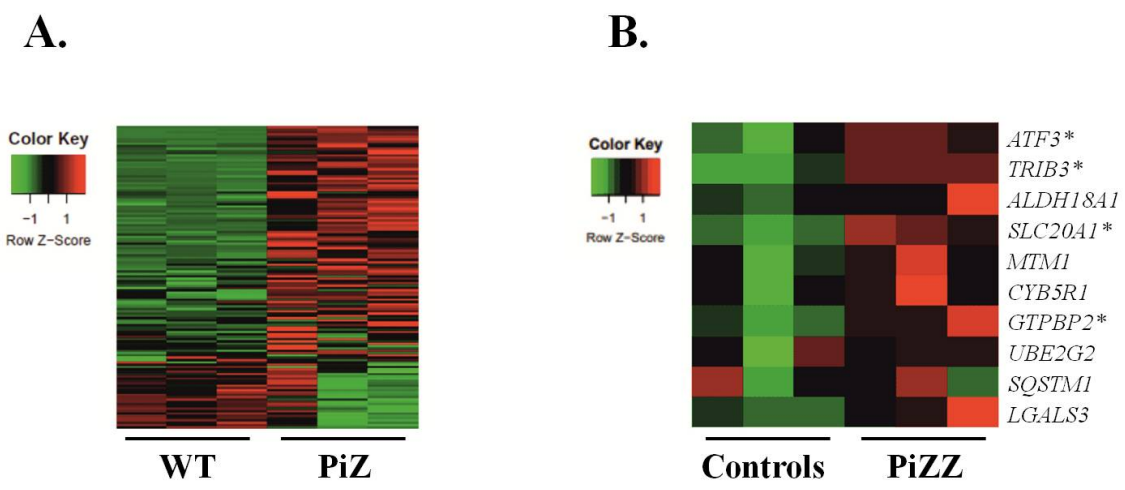

Figure 11: Up-regulation of CHOP target genes in both mouse and human livers expressing ATZ.
(**A**) Heatmap from GSEA using a set of genes up-regulated by CHOP and differentially expressed genes between 6-week-old PiZ and wild type (WT) mouse livers. The set of CHOP target genes was defined by combining ChIP-seq and RNA-seq data previously reported from tunicamycin treated WT mouse embryonic fibroblasts [103]. (**B**) Heatmap showing the expression of CHOP target genes in human liver biopsies from adult PiZZ patients with chronic liver disease and adult controls (n=3 per group; **Table 5**). *β2-MICROGLOBULIN* and *HPRT1* were used for normalization. *t*-test: *p-value<0.05.

To further investigate the relationship between ATZ and CHOP activation in liver, we injected 4-week-old PiZ mice with a recombinant serotype 8 adeno-associated viral (rAAV) vector that incorporates an artificial microRNA (miRNA) targeting the human *SERPINA*1 gene (AAV8-CB-mir914; provided by Dr. C. Mueller, UMass, Boston, USA) and results in ATZ knockdown in the liver [145]. As controls, mice were injected with the same dose of an AAV8-CB-GFP expressing the green fluorescent protein (GFP). Consistent with previous studies [145], mice injected with AAV8-CB-mir914 showed a reduction of hepatic ATZ by PAS-D staining (**Fig. 12A**), and an approximately 90% reduction of serum ATZ by 4 weeks post-injection (**Fig. 12B**). PiZ mice injected with

AAV8-CB-mir914 vector also showed a 50% reduction of *Chop* expression compared to mice injected with the control vector (**Fig. 12C**). Taken together, these data support up-regulation and activation of CHOP in human and mouse livers expressing ATZ.

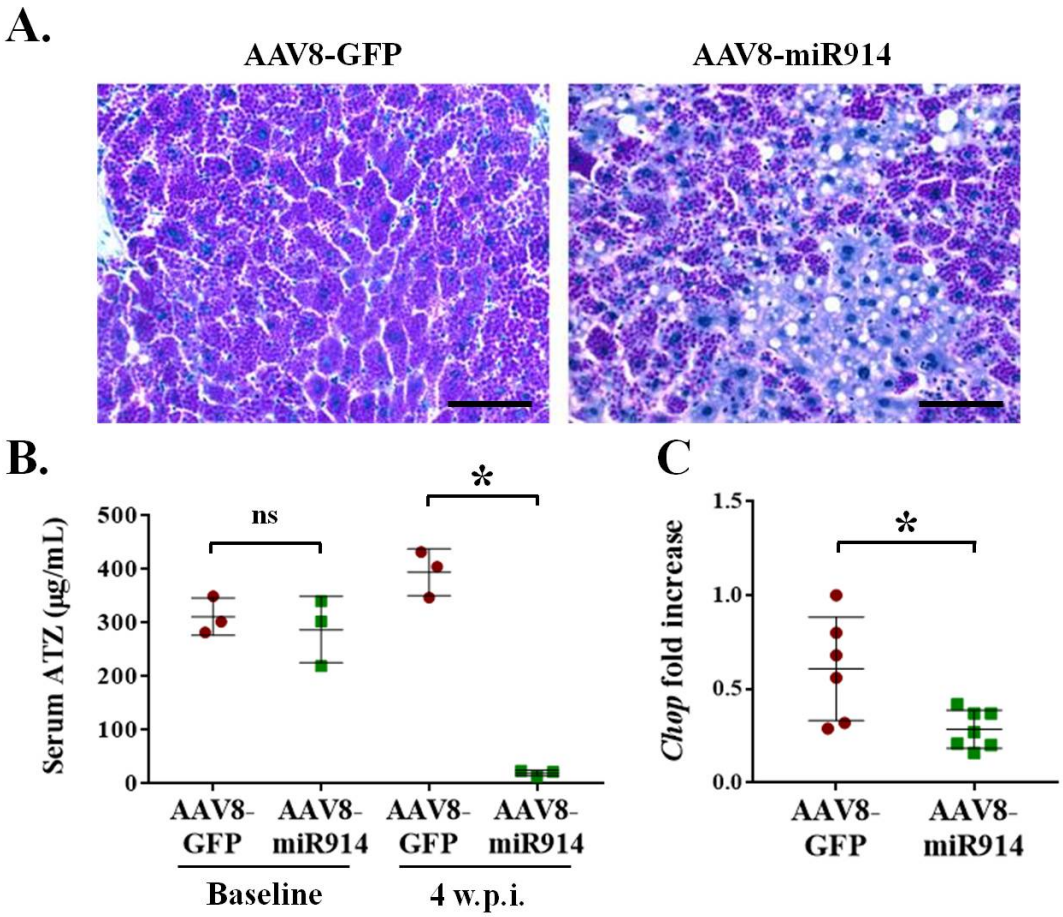

Figure 12: CHOP activation correlates with ATZ expression.
(**A**) Representative PAS-D staining on livers of PiZ mice injected with $1x10^{13}$ genome copies (gs)/Kg of recombinant serotype 8 adeno-associated viral (rAAV) vector that incorporate microRNA (miRNA) sequences targeting *SERPINA1* gene (AAV8-CB-mir914) or green fluorescent protein (GFP) as control (AAV8-CB-GFP) (20X magnification, scale bar 100 µm; at least n=5 per group). (**B**) ELISA for ATZ on serum of PiZ mice at the baseline and 4-weeks after the injection of AAV8-CB-mir914 or AAV8-CB-GFP vectors. (**C**) Real time PCR for *Chop* in livers of PiZ mice injected with AAV8-CB-mir914 or AAV8-CB-GFP vectors (at least n=5 per group). Averages ± SD are shown. *t*-test: *p-value < 0.05. Abbreviations: ns, not statistically significant; w.p.i, weeks post-injection.

4.7 Juvenile PiZ mice with deleted *Chop* have reduced hepatic accumulation of ATZ

To evaluate the role of CHOP *in vivo*, we crossed CHOP null ($Chop^{-/-}$) mice [95] with PiZ mice. $Chop^{-/-}$ mice do not exhibit a substantial phenotype unless they are subjected to stress signals [95]. PiZ mice have reduced weight compared to age- and gender-matched wild type controls [146] whereas PiZ/$Chop^{-/-}$ mice showed greater weight compared to PiZ mice (**Fig. 13A**). As previously reported [89], serum ALT levels in PiZ

mice were mildly elevated compared to controls, but they were not different from PiZ/*Chop*$^{-/-}$ mice (**Fig. 13B**).

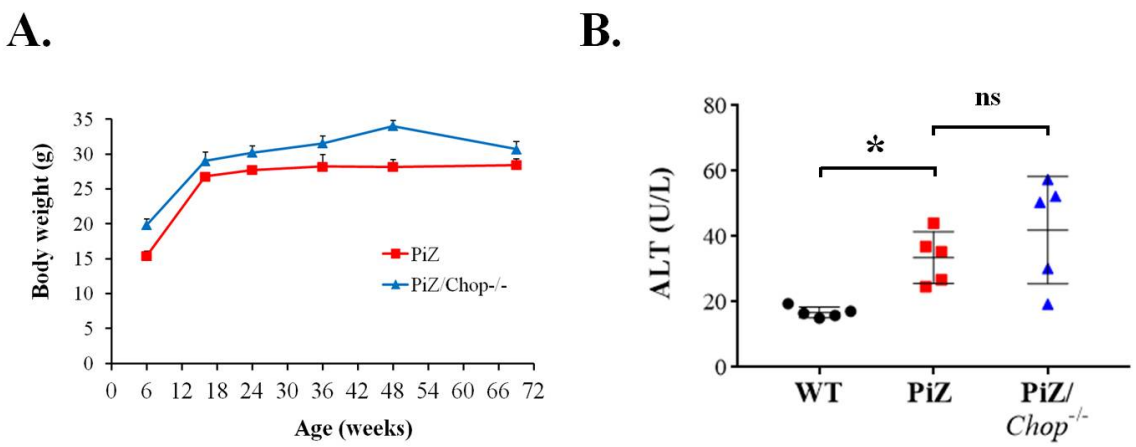

Figure 13: Alanine transaminase levels and body weight in PiZ and PiZ/*Chop*$^{-/-}$ mice.
(**A**) PiZ and PiZ/*Chop*$^{-/-}$ mice body weight at different ages (at least n=5 per group). The differences of body weights between PiZ and PiZ/*Chop*$^{-/-}$ mice were statistically significant (Time series analysis; Bayesian factor: 5.478). Averages ± SEM are shown. (**B**) Alanine transaminase (ALT) levels in the serum of 6-week-old wild type (WT), PiZ and PiZ/*Chop*$^{-/-}$ mice (n=5 per group). Averages ± standard deviations are shown. One-way ANOVA plus Tukey's post-hoc: *p-value < 0.01. Abbreviations: ns, not statistically significant.

Consistent with previous reports [147], there was no increased apoptosis in PiZ mouse livers by TUNEL assay and also PiZ/*Chop*$^{-/-}$ mice showed no increased apoptosis compared to control wild type mice (**Fig. 14**).

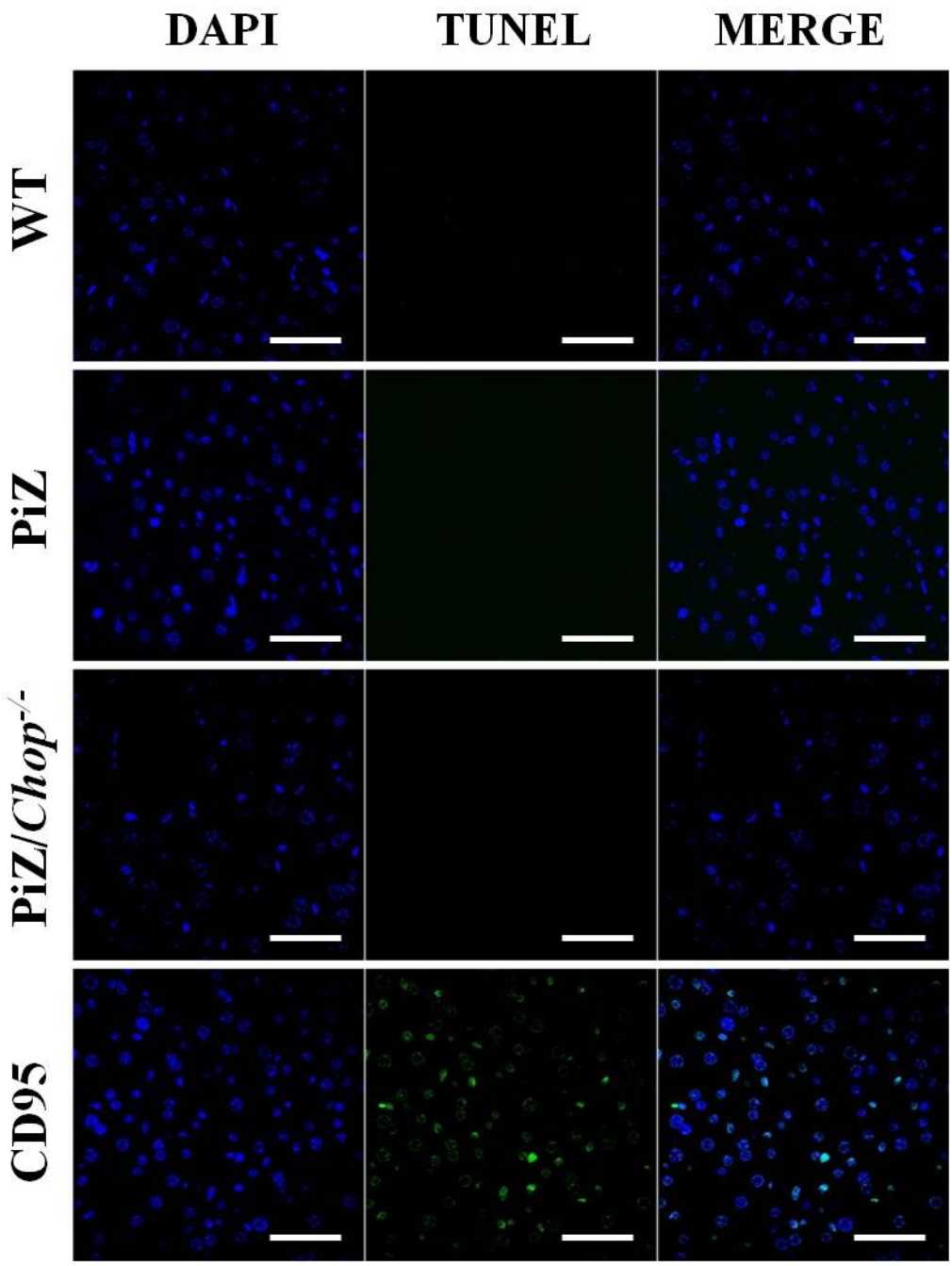

Figure 14: Apoptosis in wild type, PiZ and PiZ/*Chop*$^{-/-}$ mouse livers.
Representative TUNEL staining in 6-weeks-old wild type (WT), PiZ and PiZ/*Chop*$^{-/-}$ mouse livers (63X magnification, scale bar 50μm; n=3 per group). WT mice treated with 0.5 μg/g of body weight of CD95-activating antibody for 6 hours were used as positive control of the staining.

Serum ATZ in PiZ/*Chop*$^{-/-}$ mice was lower compared to PiZ mice at 6 weeks of age but no differences were detected in 36-week- and 69-week-old PiZ/*Chop*$^{-/-}$ compared to PiZ controls (**Fig. 15A**). Targeted qPCR analysis showed down-regulation of *SERPINA1* expression in PiZ/*Chop*$^{-/-}$ compared to age- and gender-matched 6-week-old PiZ mice and

consistent with liver ATZ content, no significant differences in *SERPINA1* expression were detected in older mice (**Fig. 15B**).

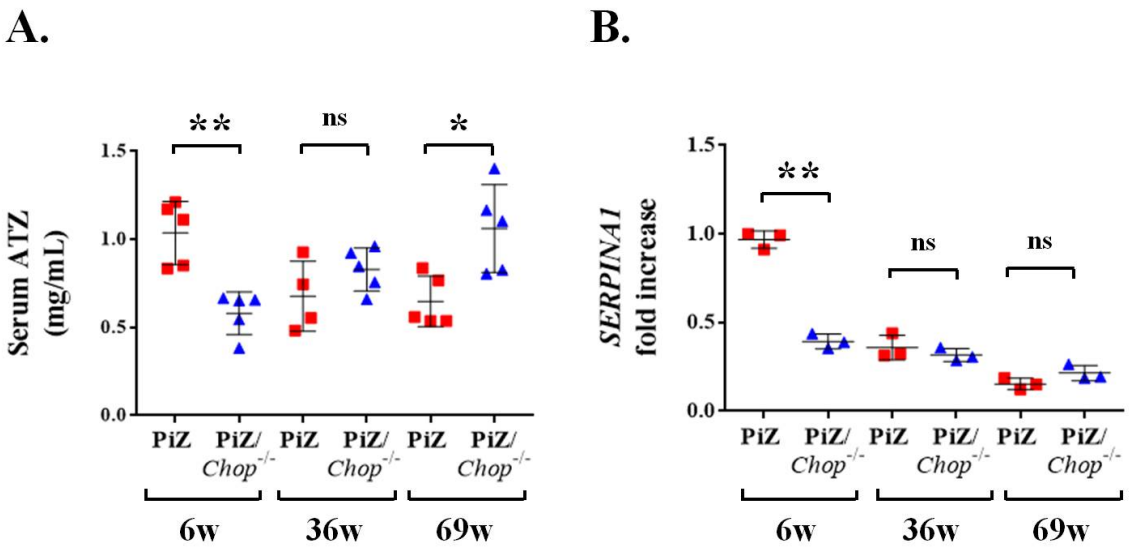

Figure 15: Deletion of *Chop* reduces serum ATZ levels and *SERPINA1* expression in juvenile PiZ mice. (**A**) ELISA for serum ATZ in PiZ and PiZ/*Chop*$^{-/-}$ mice of 6, 36, and 69 weeks of age (at least n=4 per group). Blood samples were collected from the same mice at different ages. One-way ANOVA plus Tukey's post-hoc: *p<0.05, **p<0.005. (**B**) *SERPINA1* expression in PiZ and PiZ/*Chop*$^{-/-}$ mice at 6, 36, and 69 weeks of age (n=3 per group). *β2-Microglobulin* was used for normalization. Averages ± standard deviations are shown. Two-way ANOVA plus Tukey's post-hoc: *p<0.05, **p<0.005. Abbreviations: ns, not statistically significant; 6W, 6-week-old; 36W, 36-week-old; 69W, 69-week-old.

Compared to PiZ, livers of 6-week-old PiZ/*Chop*$^{-/-}$ mice showed marked reduction of hepatic ATZ by PAS-D staining and immunofluorescence with anti-polymer antibody (**Fig. 16, 17A**). However, neither PAS-D staining nor ATZ polymer immunofluorescence detected any difference in ATZ accumulation in livers of older 36-week and 69-week-old PiZ/*Chop*$^{-/-}$ mice compared to age-matched PiZ controls (**Fig. 16, 17A-C**).

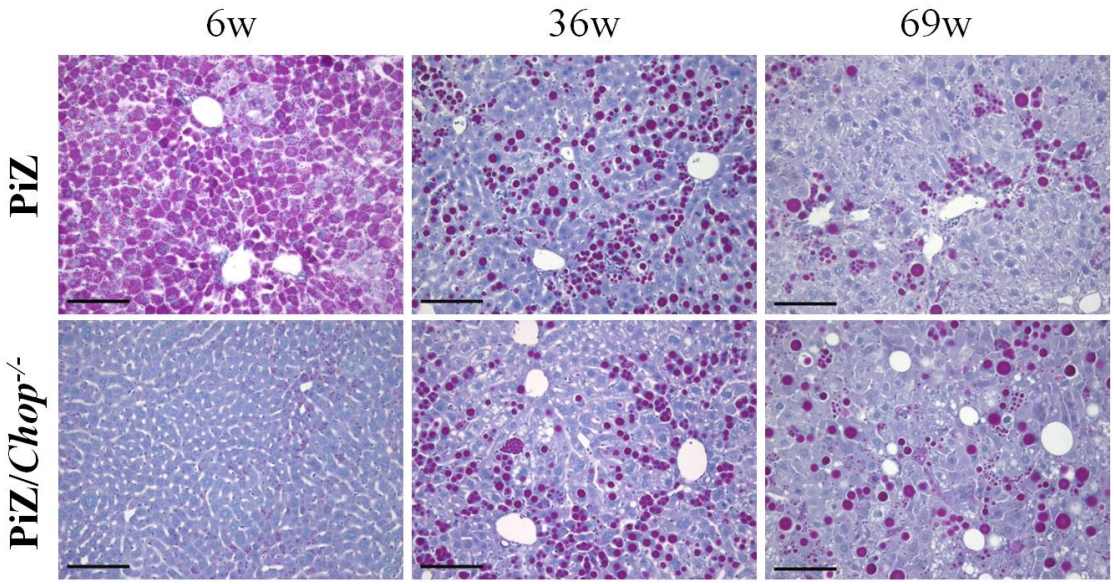

Figure 16: Genetic ablation of *Chop* reduces PAS-D positive globules in juvenile PiZ mice.
Representative PAS-D (20X magnification, scale bar 100µm) staining of livers of PiZ and PiZ/*Chop*$^{-/-}$ mice of 6, 36, and 69 weeks of age. Abbreviations: 6W, 6-week-old; 36W, 36-week-old; 69W, 69-week-old.

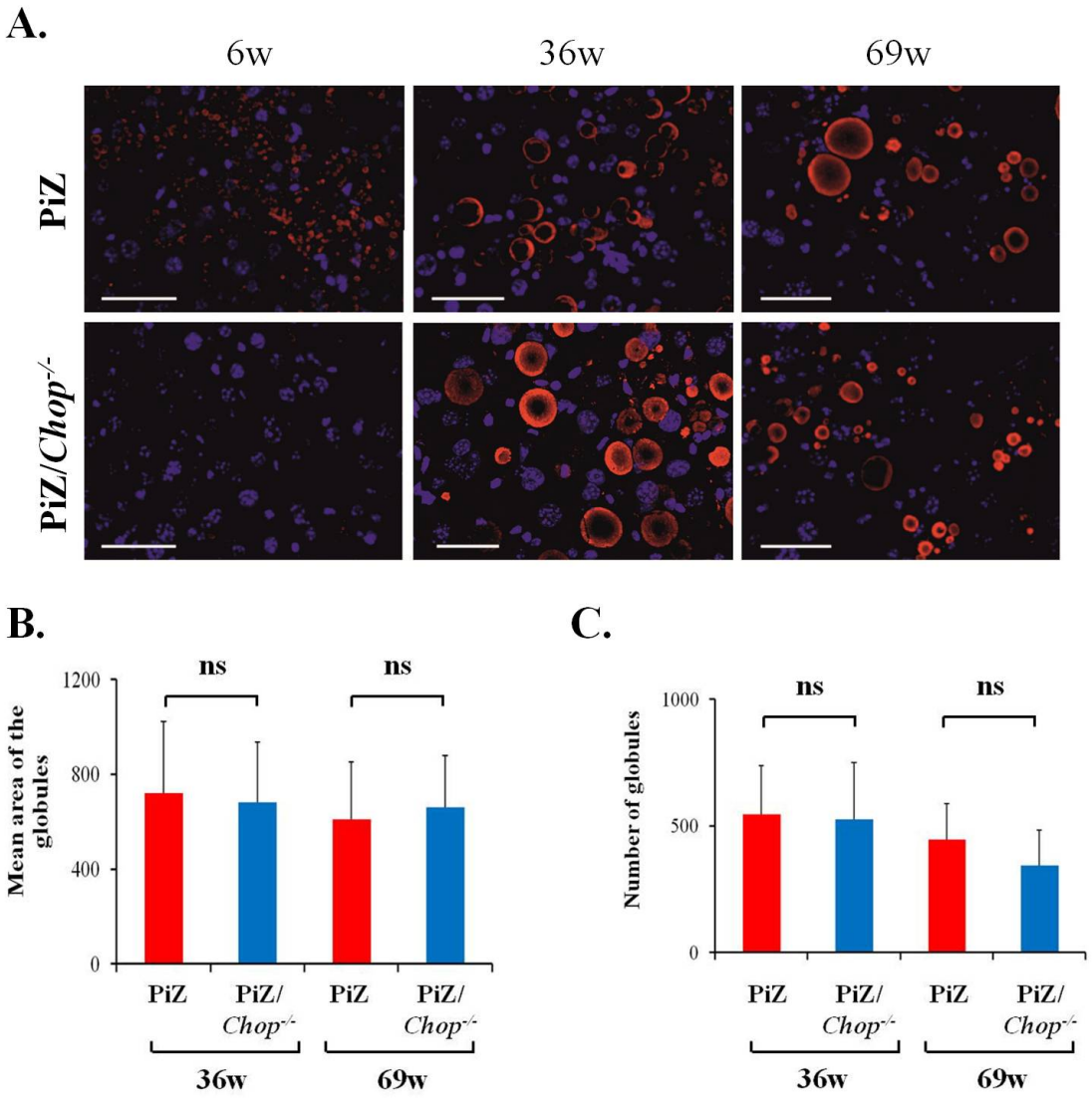

Figure 17: Genetic ablation of *Chop* reduces hepatic polymeric ATZ accumulation in PiZ mice.
(**A**) Representative immunofluorescence for polymeric ATZ (63X magnification, scale bar 50μm) of livers of PiZ and PiZ/*Chop*$^{-/-}$ mice of 6, 36, and 69 weeks of age. (**B-C**) Quantification of the mean area (**B**) and number (**C**) of the ATZ globules in 36-weeks and 69-weeks old PiZ and PiZ/*Chop*$^{-/-}$ mouse livers visualized by PAS-D staining (n=3 per group). Abbreviations: ns, not statistically significant; 6W, 6-week-old; 36W, 36-week-old; 69W, 69-week-old.

Next, I evaluated the role of CHOP in hepatic fibrosis and hepatocellular carcinoma (HCC) induced by ATZ. By real time PCR, I found that expression of genes related to liver fibrosis (*Cola1a*, *Timp-1*, *α-Sma*) were not significantly different in livers of 69-weeks old PiZ/*Chop*$^{-/-}$ mice compared to PiZ controls (**Fig. 18A**). By Sirius red staining, I also did not observe any difference in hepatic collagen deposition in 69-weeks old PiZ/*Chop*$^{-/-}$mice compared to age-matched PiZ controls (**Fig. 18B**). METAVIR score for the histopathological characterization of hepatic fibrosis and necro-inflammatory stage also confirmed that *Chop* deletion did not affect hepatic fibrosis (**Fig. 18C, D**).

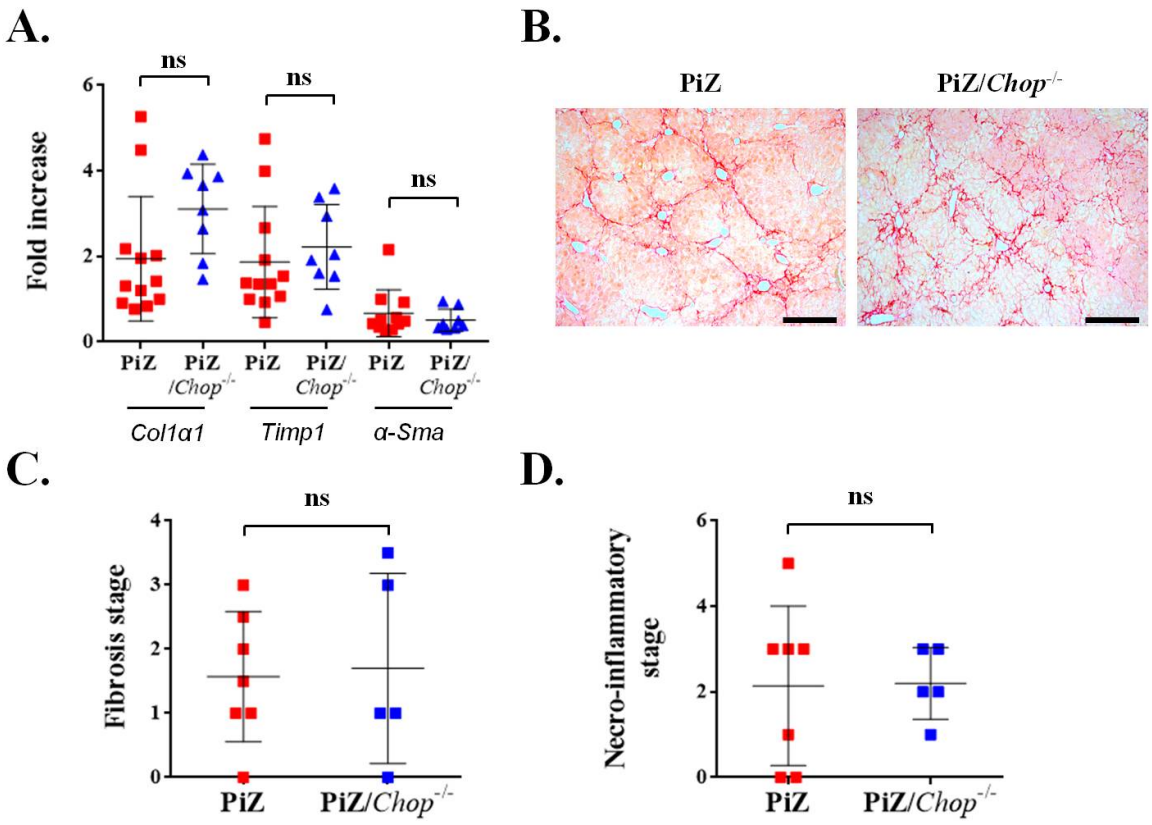

Figure 18: Genetic ablation of *Chop* did not affect hepatic fibrosis due to ATZ accumulation in PiZ mice.
(**A**) Expression of genes associated to hepatic fibrosis (*Col1α1*, *Timp1*, *α-Sma*) in PiZ and PiZ/*Chop*$^{-/-}$ mice at 69 weeks of age (at least n=5 per group). *β2-Microglobulin* was used for normalization. (**B**) Representative syrius red staining on livers of 69-weeks old PiZ and PiZ/*Chop*$^{-/-}$ mice (10X magnification, scale bar 200μm). (**C**, **D**) METAVIR score on hepatic sections from 69-weeks old PiZ and PiZ/*Chop*$^{-/-}$ mice. Averages ± standard deviations are shown. Abbreviations: ns, not statistically significant.

I also investigated the frequency of HCC in 69-weeks-old PiZ/*Chop*$^{-/-}$ and PiZ mice. I found that 3 out of 13 PiZ mice at 69 weeks of age develop HCC (about 23%) (**Fig. 19A-B**), whereas in PiZ/*Chop*$^{-/-}$ mice we found an incidence of 12.5% (2 out of 16) (**Fig. 19A-B**). Although PiZ/*Chop*$^{-/-}$ mice showed a lower HCC incidence compared to PiZ controls, the number of animals used in this experiment is not sufficient to achieve a statistically significance and thus, further studies are needed to investigate whether *Chop* deletion reduces the frequency of HCC in PiZ mice.

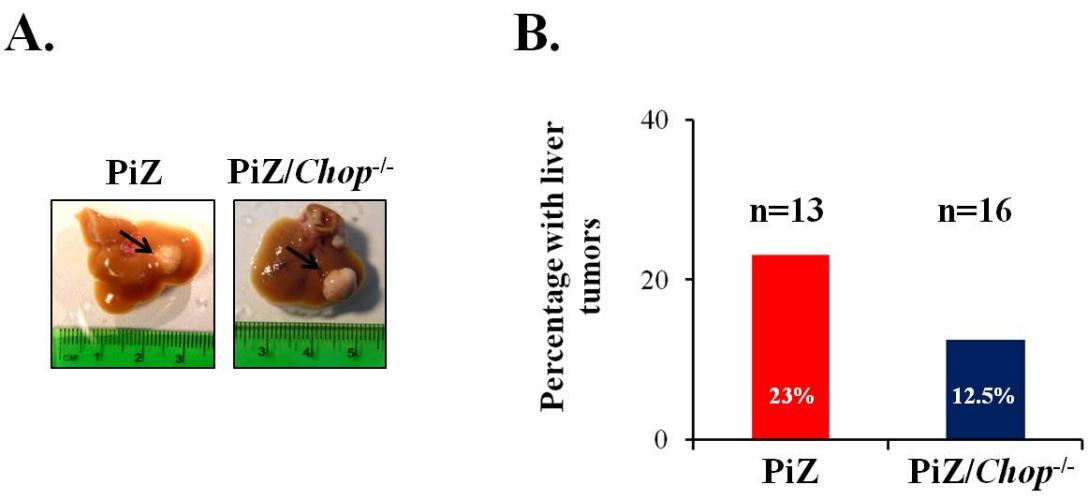

Figure 19: HCC incidence was not affected by *Chop* deletion in PiZ mice.
(**A**) Representative liver photos derived from 69-weeks-old PiZ and PiZ/*Chop*$^{-/-}$ mice. Tumoral nodules are indicated by black arrows. (**B**) Incidence of liver tumors in 69-weeks-old PiZ and PiZ/*Chop*$^{-/-}$ mice (n=13 PiZ, n=16 PiZ/*Chop*$^{-/-}$).

To investigate the mechanism underlying reduced accumulation of ATZ in 6-week-old PiZ/*Chop*$^{-/-}$ mice, we evaluated protein ubiquitination and LC3-II to rule out the involvement of UPS and autophagy. However, no differences were detected between PiZ and PiZ/*Chop*$^{-/-}$ mice (**Fig. 20**), suggesting that other mechanisms are involved in determining different degree of ATZ accumulation.

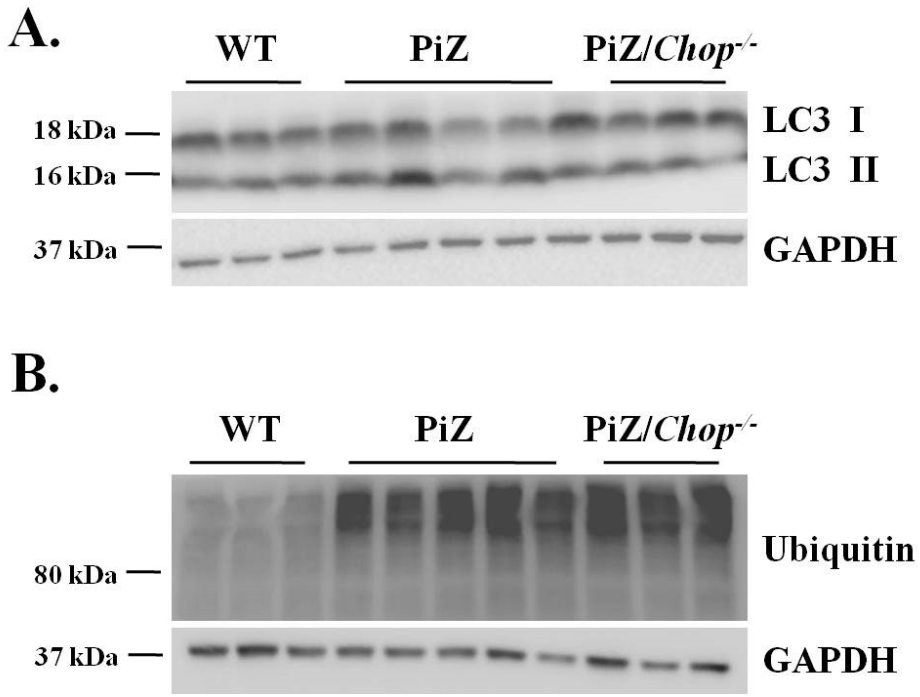

Figure 20: Autophagy marker LC3 and ubiquitin levels are not affected by *Chop* deletion.
(**A**) Western blotting of LC3-I and LC3-II in wild type (WT), PiZ and PiZ/*Chop*$^{-/-}$ mouse livers at 6 weeks of age. GAPDH was used for normalization. (**B**) Western blotting of total ubiquitinated proteins in WT, PiZ and PiZ/*Chop*$^{-/-}$ mouse livers at 6 weeks of age. GAPDH was used for normalization. Abbreviations: GAPDH, glyceraldehydes 3-phosphate dehydrogenase.

Altogether these data suggest that genetic ablation of *Chop* reduces hepatic ATZ accumulation in juvenile PiZ mouse livers. Deletion of *Chop* did not affect liver fibrosis and does not seem to affect significantly the frequency of HCC although further studies with larger number of mice are needed to draw a firm conclusion. Finally, these findings suggest a role of CHOP in transcriptional regulation of *SERPINA1* in juvenile PiZ livers.

4.8 Complexes of CHOP with C/EBPβ or c-JUN up-regulate SERPINA1

SERPINA1 contains regulatory elements both at 5' (**Fig. 21A**) and 3'UTR [30]. The 5'UTR contains putative binding sites for the AP-1 (in green in **Fig. 21A**), CHOP-C/EBPβ heterodimers (in red in **Fig. 21A**) and C/EBPβ homodimers (in blue in **Fig. 21A**) [30]. In addition, we also found putative binding sites for C/EBPβ-CHOP heterodimers (in red in **Fig. 4.21A**). CHOP can make stable heterodimers with AP-1 complex (e.g. c-JUN and c-FOS) and C/EBPβ [148, 149]. To investigate how CHOP regulates *SERPINA1* expression,

I co-transfected HeLa cells with a plasmid expressing CHOP and the pAAT-Luc-AAT-3'UTR plasmid that contains the *SERPINA1* regulatory elements included in PiZ transgenic mice [109] (dashed line in **Fig. 21A**) upstream the *firefly luciferase* coding region and *SERPINA1* 3'UTR. As positive control, cells were co-transfected with a plasmid expressing c-JUN that transactivates luciferase activity, as previously shown in **Fig. 7** (**Fig. 21B**). Compared to cells co-transfected with the negative control, cells co-transfected with CHOP showed a mild increase in luciferase levels, suggesting that CHOP is sufficient to up-regulate *SERPINA1* expression (**Fig. 21B**). In contrast, transfections of plasmids expressing c-FOS or C/EBPβ did not increase luciferase activity (**Fig. 21B**). Co-transfection of CHOP and c-JUN resulted in greater increase of luciferase levels compared to cells transfected with plasmids expressing each of the two transcription factors alone (**Fig. 21B**). Co-transfection of CHOP and C/EBPβ also resulted in greater increase of luciferase levels compared to cells transfected with the plasmid expressing CHOP (**Fig. 21B**). Mutagenesis of the binding site 2 of the CHOP-C/EBPβ and, at a lower extent, of the binding site 1 (in red in **Fig. 21A**) reduced luciferase activity (**Fig. 21C**). Mutagenesis of the binding site 2 but not site 1 of the AP-1 binding site (in green in **Fig. 21A**) reduced luciferase activity (**Fig. 20C**). Taken together, these results show that site 2 of the CHOP-C/EBPβ putative binding site is required for transactivation by CHOP and C/EBPβ and site 2 of the AP-1 binding site is required for transactivation by CHOP and c-JUN.

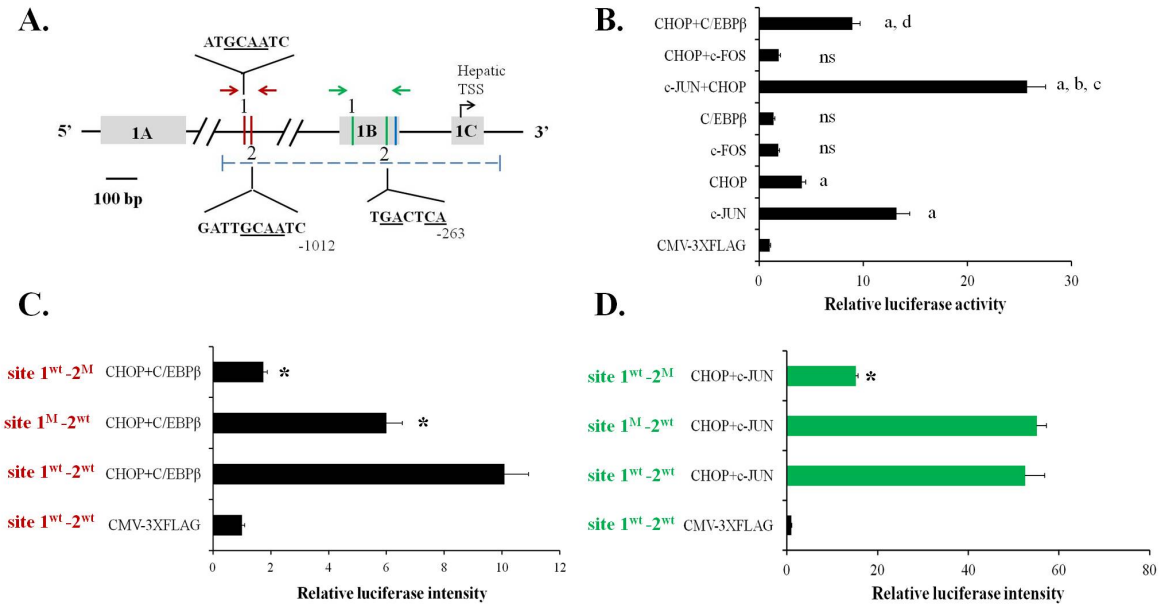

Figure 21: c-JUN-CHOP and C/EBPβ-CHOP complexes up-regulate *SERPINA1* expression.
(**A**) Schematic representation of the AP-1 binding sites (1 and 2; in green), putative C/EBPβ-CHOP heterodimer binding sites (1 and 2; in red) and putative C/EBPβ binding site (in blue) in the 5'untraslated region (UTR) of the *SERPINA1* gene (drawn to scale). Nucleotide sequences are shown for the binding sites confirmed by luciferase assays: sites 1 and 2 for C/EBPβ-CHOP heterodimer and site 2 for c-JUN-CHOP heterodimer. Nucleotide numbering is calculated as distance from the hepatic TSS. Arrows indicate the position of the primers for the qPCR on the liver chromatin immunoprecipitates. The dashed line indicates the promoter region cloned upstream the *luciferase* reporter gene in the pAAT-Luc-AAT-3'UTR plasmid. Underlined nucleotides have been mutagenized. (**B**) Luciferase activity in HeLa cells co-transfected with the pAAT-Luc-AAT-3'UTR construct and the plasmids expressing human CHOP, C/EBPβ, c-JUN, c-FOS or their combinations. An empty CMV-3XFLAG plasmid was used as control. Averages ± standard deviations are shown. One-way ANOVA plus Tukey's post-hoc: a: *p-value < 0.001 vs CMV-3XFLAG; b: *p-value < 0.0001 vs c-JUN; c: *p-value < 0.0001 vs CHOP. d: *p-value < 0.05 vs CHOP. (**C-D**) Luciferase activity in HeLa cells co-transfected with the pAAT-Luc-AAT-3'UTR construct and with mutagenized sites 1 and 2 of CHOP-C/EBPβ or AP-1 binding sites and the plasmids expressing human CHOP and C/EBPβ or c-JUN. An empty CMV-3XFLAG plasmid was used as control. One-way ANOVA plus Tukey's post-hoc: *p-value < 0.0001 vs site 1^{WT}-2^{WT} CHOP + C/EBPβ (**C**) or vs 1^{WT}-2^{WT} CHOP + c-JUN (**D**). Abbreviations: ns, not statistically significant;

Protein co-immunoprecipitation in HeLa cells co-transfected with a plasmid expressing CHOP-FLAG and c-JUN-MYC or C/EBPβ showed that CHOP binds c-JUN (**Fig. 22A**) and all three isoforms of C/EBPβ (LAP*, LAP and LIP) (**Fig. 22B**) consistent with previous studies [149-152].

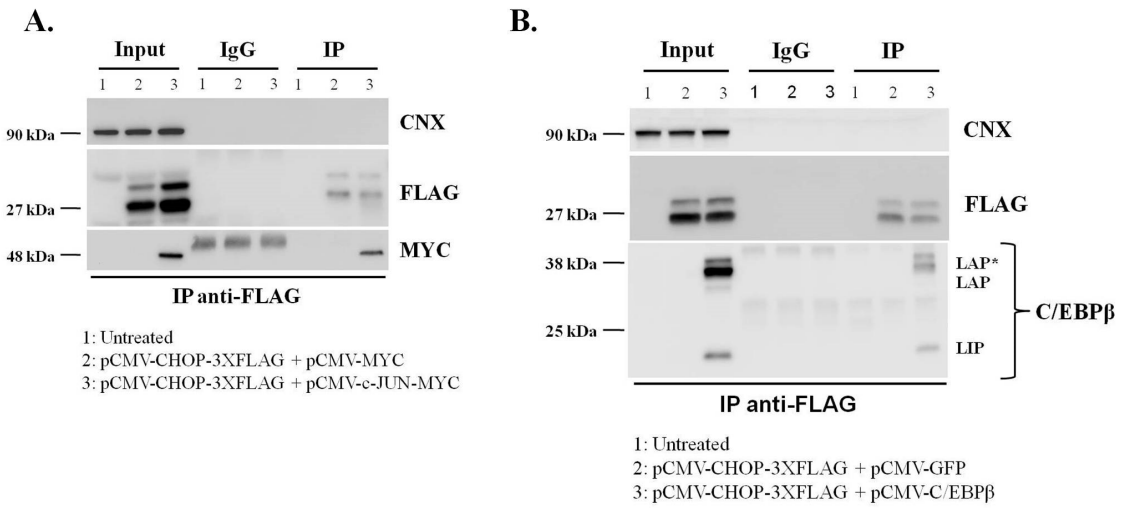

Figure 22: CHOP co-immunoprecipitates with c-JUN and C/EBPβ.
(**A**) HeLa cells were transfected with plasmids expressing CHOP-3XFLAG and c-JUN-MYC fusion proteins or control vector (p-CMV-MYC) or left untreated. Cell lysates were immunoprecipitated with anti-FLAG antibody and immunoblotted with anti-FLAG antibody to detect CHOP-3XFLAG and anti-MYC antibody to detect c-JUN-MYC. Calnexin (CNX) was used as protein loading control. Anti-FLAG immunoblotting displayed two bands corresponding the two CHOP isoforms arising from differential translation initiation. (**B**) HeLa cells were transfected with plasmids expressing CHOP-3XFLAG fusion protein and C/EBPβ or control vector (pCMV-GFP) or left untreated. Cell lysates were immunoprecipitated with anti-FLAG antibody and immunoblotted with anti-FLAG antibody to detect CHOP-3XFLAG and anti-C/EBPβ antibody. CNX was used as protein loading control. Anti-FLAG immunoblotting displayed two bands corresponding by the two CHOP isoforms arising from differential translation initiation. Abbreviations: CNX, calnexin; IP, immunoprecipitates.

To investigate the binding of CHOP, c-JUN and C-EBPβ to *SERPINA1* regulatory elements, we performed ChIP on PiZ mouse livers with anti-phospho-c-JUN, anti-C/EBPβ, or anti-CHOP antibodies. Consistent with findings shown in section 1, enrichment of AP-1 binding sites (in green in **Fig. 23A**) was detected in the immunoprecipitates with anti-phospho-c-JUN antibody whereas no significant enrichment was detected for the putative CHOP-C/EBPβ binding sites (in red in **Fig. 23A**). No enrichment was detected for *Gapdh* promoter region used as negative control (**Fig. 23A**). In the ChIP with anti-C/EBPβ antibody, no enrichment was found for putative CHOP-C/EBPβ binding sites (in red in **Fig. 23B**), AP-1 binding sites (in green in **Fig. 23B**) and putative C/EBPβ binding sites (in blue in **Fig. 23B**) whereas two positive control regions of *Gabarapl1* and *Ctsl1* promoters were both enriched (**Fig. 23B**).

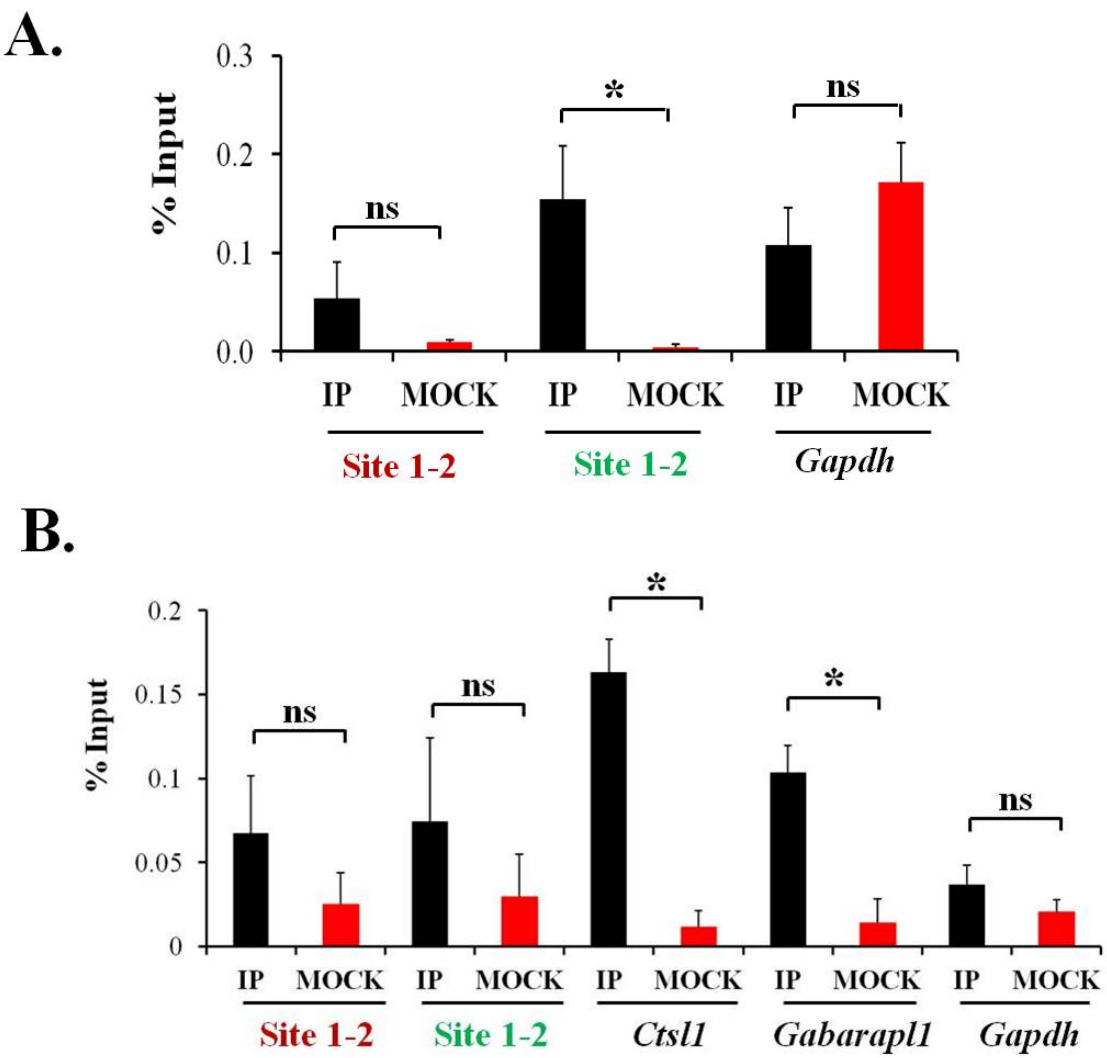

Figure 23: Chromatin immunoprecipitations in PiZ mouse livers showing the binding of c-JUN on the AP-1 binding sites of the *SERPINA1* 5'UTR.
(**A-B**) Chromatin immunoprecipitation (ChIP) on PiZ mouse livers using anti-phospho-c-JUN (A) and anti-C/EBPβ (B) antibodies followed by qPCR on CHOP-C/EBPβ (in red) and CHOP/c-JUN (in green) putative binding sites. *Ctsl1* and *Gabarapl1* promoter regions were amplified as positive control for C/EBPβ enrichment. *Gapdh* was used as negative control. Averages ± standard deviations are shown. *t*-test: *p-value < 0.05. Abbreviations: IP, immunoprecipitated; ns, not statistically significant.

Finally, by ChIP with anti-CHOP antibody, CHOP-C/EBPβ binding sites (in red in **Fig. 21A**) were significantly enriched in PiZ mouse livers whereas no enrichment was detected for AP-1 binding sites (in green in **Fig. 21A**) (**Fig. 24A**). As positive control of the ChIP with anti-CHOP antibody, *p62* promoter region was found to be enriched in PiZ livers whereas no signal was detected for the *Rpl30* promoter used as negative control. Both CHOP-C/EBPβ binding sites and p62 promoter region were not enriched by ChIP with anti-CHOP antibody in PiZ/*Chop*$^{-/-}$ mouse livers (**Fig. 24B**). Altogether, these results show

that CHOP binds the CHOP-C/EBPβ binding sites while phospho-c-JUN binds AP-1 binding sites in the 5' UTR region of the *SERPINA1* gene. C/EBPβ was not found to directly bind the *SERPINA1* regulatory regions but protein-protein interactions are lost in the ChIP experiment and the luciferase and immunoprecipitation data suggest that C/EBPβ forms a complex with CHOP on the CHOP-C/EBPβ binding sites.

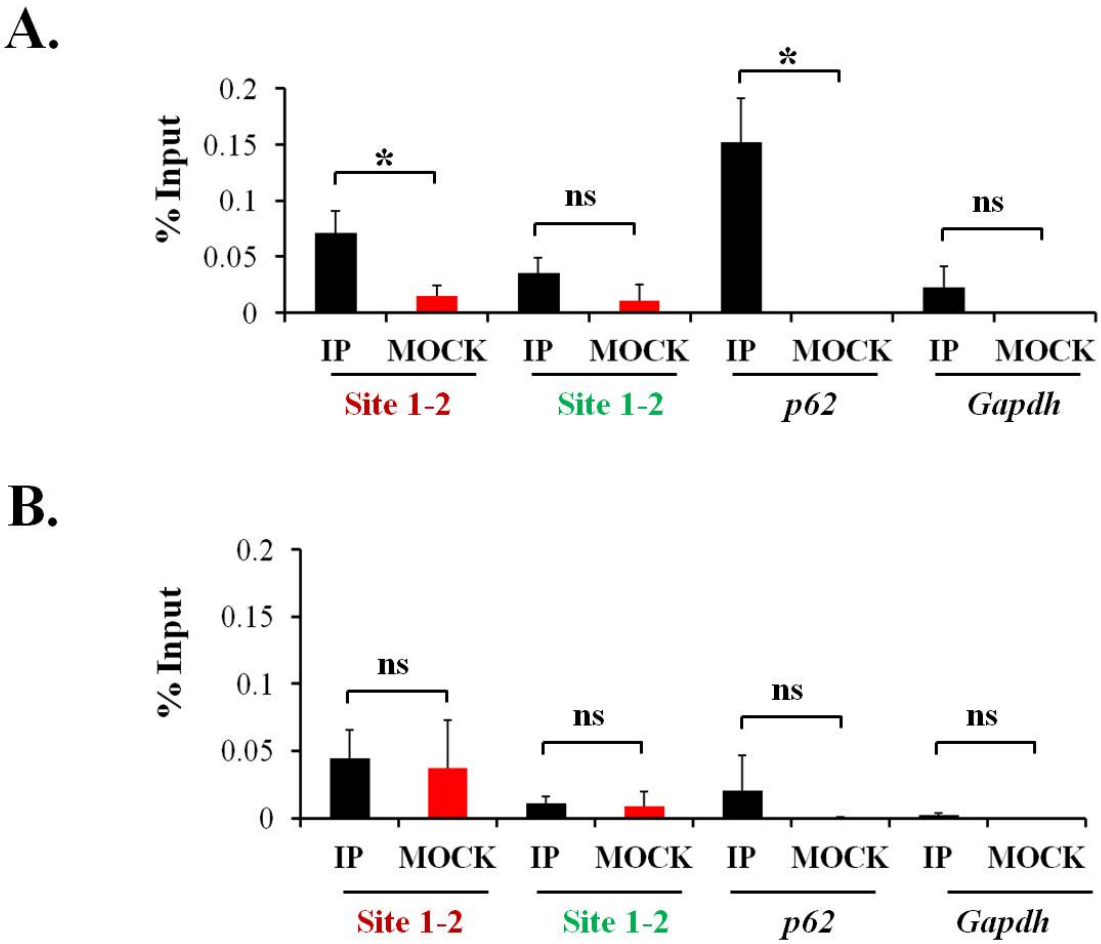

Figure 24: CHOP binds the CHOP-C/EBPβ binding sites in the 5'UTR of the *SERPINA1*.
(**A**) Chromatin immunoprecipitations (ChIP) on PiZ mouse livers with anti-CHOP antibody: CHOP/C-EBPβ binding sites 1 and 2 were significantly enriched. *p62* and *Rpl30* promoter regions were used as positive and negative controls respectively. (**B**) Chromatin immunoprecipitations (ChIP) on PiZ/*Chop*$^{-/-}$ mouse livers with anti-CHOP antibody: CHOP/C-EBPβ binding sites 1 and 2, AP-1 binding sites, *p62* and *Rpl30* promoter regions showed no enrichment consistently with the lack of CHOP in these mice. Averages ± standard deviations are shown. *t*-test: *p-value < 0.05. Abbreviations: IP, immunoprecipitated; ns, not statistically significant.

Next, I investigated the contribution of each of the two CHOP-C/EBPβ putative binding sites in CHOP/c-JUN complex-mediated transactivation of *SERPINA1*. HeLa cells were co-transfected with plasmids expressing CHOP and c-JUN, and with the pAAT-Luc-AAT-3'UTR plasmid including either the wild type sequences or mutagenized putative

CHOP-C/EBPβ binding sites (in red in **Fig. 21A**). pAAT-Luc-AAT-3'UTR bearing mutated CHOP/c-JUN binding sites were transfected as controls. Consistent with the co-transfection of CHOP and C/EBPβ (**Fig. 21C**), mutagenized CHOP-C/EBPβ binding site 1 resulted in moderate but significant reduction of luciferase activity in cells co-transfected with CHOP and c-JUN (**Fig. 25**). Mutagenized site 2 instead completely abolished CHOP and c-JUN transactivation (**Fig. 25**) and resulted in lower luciferase activity compared to cells transfected with the pAAT-Luc-AAT-3'UTR plasmid including the wild type sequences (**Fig. 25**). These findings suggest that binding of CHOP to CHOP-C/EBPβ site 2 (in red in **Fig. 21A**) is essential for *SERPINA1* expression induced by CHOP and c-JUN.

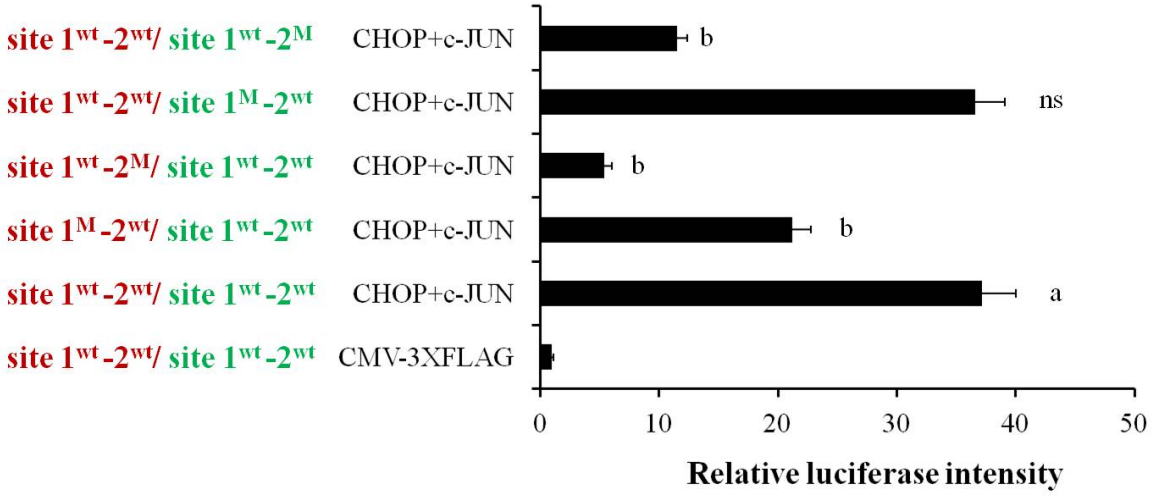

Figure 25: Mutations in the C/EBPβ-CHOP binding sites reduce the CHOP/c-JUN dependent transactivation of *SERPINA1* expression.
Luciferase activity in HeLa cells co-transfected with the pAAT-Luc-AAT-3'UTR construct, constructs with mutagenized sites 1 and 2 of CHOP-C/EBPβ or AP-1 binding sites and the plasmids expressing human CHOP and c-JUN. An empty CMV-3XFLAG plasmid was used as control. Averages ± standard deviations are shown. One-way ANOVA plus Tukey's post-hoc: a: *p-value < 0.001 vs CMV-3XFLAG; b: *p-value < 0.001 1^{WT}-2^{WT}/1^{WT}-2^{WT} CHOP+c-JUN. Abbreviations: ns, not statistically significant.

Chapter 5: Discussion

JNK signaling in AATD-related liver disease

The main finding of data presented in section 1 of Chapter 4 is that JNK and c-JUN play an important role in liver disease due to toxic accumulation of ATZ by promoting *SERPINA1* transcriptional up-regulation. I showed that JNK is activated in mouse and human livers and being a direct target of JNK1/2, c-JUN regulates *SERPINA1* expression. I found that the lack of either JNK1 or JNK2 resulted in reduced c-JUN activation and *SERPINA1* expression, thus reducing hepatic ATZ accumulation.

Most patients homozygous for the Z mutation never develop clinically relevant liver disease. The development of liver injury is thought to require environmental or genetic factors that in addition to the Z mutation can reach the threshold for intracellular accumulation and toxicity. The results of these studies suggest that JNK is an important player which regulates the toxicity of proteotoxic mutant ATZ.

JNKs are important signaling molecules in multiple pathways in liver physiology and diseases. JNK activation affects important biologic functions, such as liver regeneration but the same signaling pathway can also be detrimental, such in carcinogenesis [153]. The transcription factor c-JUN is a direct target of JNK and was found to be activated and increased in the nuclear extracts of PiZ livers. *SERPINA1* was previously found to contain two putative binding sites for AP-1 [30], composed of c-FOS and c-JUN [116]. The luciferase assay in HeLa cells co-transfected with the human c-JUN and with the AP-1 consensus sequences of the *SERPINA1* and the ChIP study indeed confirmed c-JUN trans-activation of *SERPINA1* in PIZ mouse livers.

AAT is an acute-phase protein, controlled by several cytokines, such as IL-6, IL-1β, TNF-α, oncostatin M or bacterial lipopolysaccharide [30, 154]. Interestingly, c-JUN up-regulates IL-6 and TNF-α expression [155, 156] and thus, it can also indirectly increase *SERPINA1* expression by increasing cytokine levels.

Based on the data I generated, factors acting on the JNK pathway such as concomitant inflammatory states might further increase *SERPINA1* transcription to reach the threshold of toxicity for the development of liver disease in AAT deficiency. Additionally, genetic modifiers, including those that modulate protein degradation or those that could be directly injurious to the liver might be also involved in achieving the toxicity threshold.

Although its involvement in livers expressing ATZ is controversial [65, 157-159], the unfolded protein response can be responsible for JNK activation [111, 160]. Nevertheless, the factor(s) activating JNK remains to be investigated.

The liver disease of AAT deficiency predisposes to HCC [14]. Several clinical and experimental studies have implicated stress-activated MAPK cascades that converge on JNK and p38 as key regulators of hepatocarcinogenesis [161, 162]. Hepatitis C and nonalcoholic steatohepatitis which are predisposing factors for HCC both involve JNK activity. JNK1 and JNK2 are phosphorylated in samples from patients with primary HCC [163]. JNK1 down-regulates transcription of *p21* via c-MYC [163] and c-JUN promotes hepatocarcinogenesis by antogonizing p53 activity [164]. Moreover, *c-JUN* deletion in mouse hepatocytes reduces the frequency of HCC [163]. Therefore, our findings of activated JNK and c-JUN in livers expressing ATZ are relevant to understand the cancer progression in AAT deficiency.

From a therapeutic perspective, it will be of great importance to understand how JNK pathway could be pharmacologically manipulated to improve the liver disease of AAT deficiency. We found that inhibition of JNK might have therapeutic potential in patients homozygous for the Z mutation. However, JNK molecules play important roles in a large number of cellular processes and their inhibition could result in significant side effects. Nevertheless, understanding cross-talk among JNK and other pathways activated in livers expressing ATZ as well as how these activities are linked with inflammation should provide new treatment and prevention strategies. In conclusion, our findings elucidate an important pathway involved in the pathogenesis of liver disease in patients homozygous

for the Z mutation and highlight novel therapeutic targets.

Role of the transcription factor CHOP in AATD-related liver disease

Like c-JUN, I have also found that the transcription factor CHOP plays an important role in determining the severity of liver disease due to ATZ. It is up-regulated and activated in livers of PiZ mice and PiZZ patients and juvenile *Chop*-deleted mice show marked reduction of liver ATZ accumulation. Finally, I found that CHOP is involved in regulation of *SERPINA1* and I identified the sites of binding of CHOP on *SERPINA1* promoter.

Although it has been involved in the pathogenesis of several liver disorders [165], the role of CHOP in the hepatic disease induced by ATZ has not been yet recognized. CHOP is an important player in the unfolded protein response and ER-stress response. Moreover, it is activated by several stimuli, such as amino acid and glucose deprivation, DNA damage, cellular growth arrest and hypoxia [166]. While the precise factors activating CHOP in livers expressing ATZ remain to be identified, we found that CHOP up-regulation plays an important role in aggravating ATZ accumulation in juvenile PiZ mice through transcriptional up-regulation of *SERPINA1* expression. CHOP is a member of the C/EBP transcription factors that bind to the CCAAT box motif present in several promoters. It includes transcriptional activation/repression domains at its N-terminus and a C-terminus bZIP domain that mediates sequence-specific DNA binding and dimerization. Consistent with previous studies [148, 150, 152], CHOP was found to form complexes with C/EBPβ and c-JUN and these complexes enhanced *SERPINA1* expression. I also showed that CHOP binds the promoter region and up-regulates *SERPINA1* but also greatly enhances c-JUN-mediated transcriptional up-regulation of *SERPINA1*. CHOP has indeed a pivotal role in *SERPINA1* up-regulation because the lack of CHOP binding to *SERPINA1* promoter greatly diminished *SERPINA1* expression induced by c-JUN binding to a distinct site. It was previously proposed that CHOP enhances the transcriptional activation of AP-1 by

tethering to the AP-1 complex without direct binding of DNA [149]. Our findings suggest that transcriptional activation of AP-1 can also occur with binding of CHOP to a site located closed to the AP-1 site, because *SERPINA1* transcriptional activation was greatly diminished when the CHOP/C-EBPβ binding site was mutagenized.

Previous data showed that CHOP and c-JUN also cooperatively mediate the induction of PUMA (p53 up-regulated modulator of apoptosis) during hepatocyte lipoapoptosis [167]. More broadly, these data raise the question of whether CHOP potentiates c-JUN-mediated transcription in other cell types under different physiologic and disease conditions. Interestingly, CHOP is transcriptionally positively regulated by the AP-1 complex [135] suggesting a feedback positive loop, in which c-JUN activation up-regulates CHOP whereas CHOP activation in turn further enhances *SERPINA1* expression. Such feed-forward mechanism results in ATZ overload and worsening of the liver disease.

In contrast to older mice, juvenile PiZ mice deleted for *Chop* showed marked reduction of ATZ accumulation suggesting a different role of CHOP at different disease stages. Interestingly, levels of blood ATZ in PiZZ patients also appear to decline over time [168], a finding that parallels the mouse data shown in this and previous studies [74]. The mechanisms underlying the age dependent reduction of CHOP are unknown but the reduced load of ATZ due to decreased HNF-4α is a possible explanation [169].

Clinical data suggest that the human disease has different features in infants compared to adults. A survey of large transplantation databases suggested that AAT deficiency most commonly causes liver disease requiring liver transplantation in adults, but it also revealed that almost all transplant in children were performed under the age of 5 years [18]. These differences suggest that pathogenetic mechanisms vary depending on the age and more powerful modifiers play a role in the liver disease in children [18]. Based on my findings, I propose that CHOP and factors regulating its expression might be among the modifiers responsible for the more severe disease occurring in the pediatric population. Interestingly, CHOP is up-regulated by non-steroidal anti-inflammatory drugs (NSAIDs)

[170] and indomethacin given to PiZ mice was previously shown to increase hepatic injury and *SERPINA1* expression resulting in greater accumulation of ATZ [171]. Moreover, exposure of hepatocytes to acetaminophen activates JNK and CHOP and genetic ablation of *Chop* and *Jnk2* prevents acetaminophen-induced liver injury [172, 173]. Therefore, environmental factors, including drugs, could aggravate ATZ-induced liver injury and NSAIDs may be particularly dangerous in children with AAT deficiency.

There is currently no therapeutic option for children with liver failure due to ATZ except for liver transplantation. My studies suggest that inhibition of CHOP might be therapeutically relevant in children with severe disease progressing to liver failure and requiring liver transplantation.

Given its recognized role in promoting liver fibrosis and HCC [174-176] which are important complications of ATZ-induced liver disease, CHOP might play a role in these complications. However, further studies are needed to address these issues.

In summary, my studies suggest that CHOP is an important player in aggravating liver toxicity from abundant accumulation of toxic ATZ in juvenile mice and patients. Drugs inhibiting CHOP activity might have potential for therapy of acute liver failure in children.

In conclusion, I propose a model in which hepatocytes expressing ATZ have increased activation of JNK/c-JUN and CHOP signaling pathways and as a consequence of a feedback positive loop, they further increase *SERPINA1* transcription aggravating ATZ accumulation (**Fig. 26**). To address the factors involved in the pathogenesis of the liver disease, most studies have been focused on ATZ protein degradation by the ubiquitin-proteasome system or autophagy [177] whereas the contribution of transcriptional regulation of *SERPINA1* expression has been neglected. In the livers of subjects carrying the Z allele, increased synthesis of ATZ augments the burden of mutant protein and proteotoxicity leading to liver disease. Thus, the understanding of factors involved in the regulation of *SERPINA1* expression in both physiological and pathological conditions is

extremely important to identify new therapeutic targets. The findings of my studies might ultimate provide new therapeutic and preventive targets for therapy of liver disease due to ATZ by elucidation of pathogenic mechanisms affecting *SERPINA1* expression during liver injury.

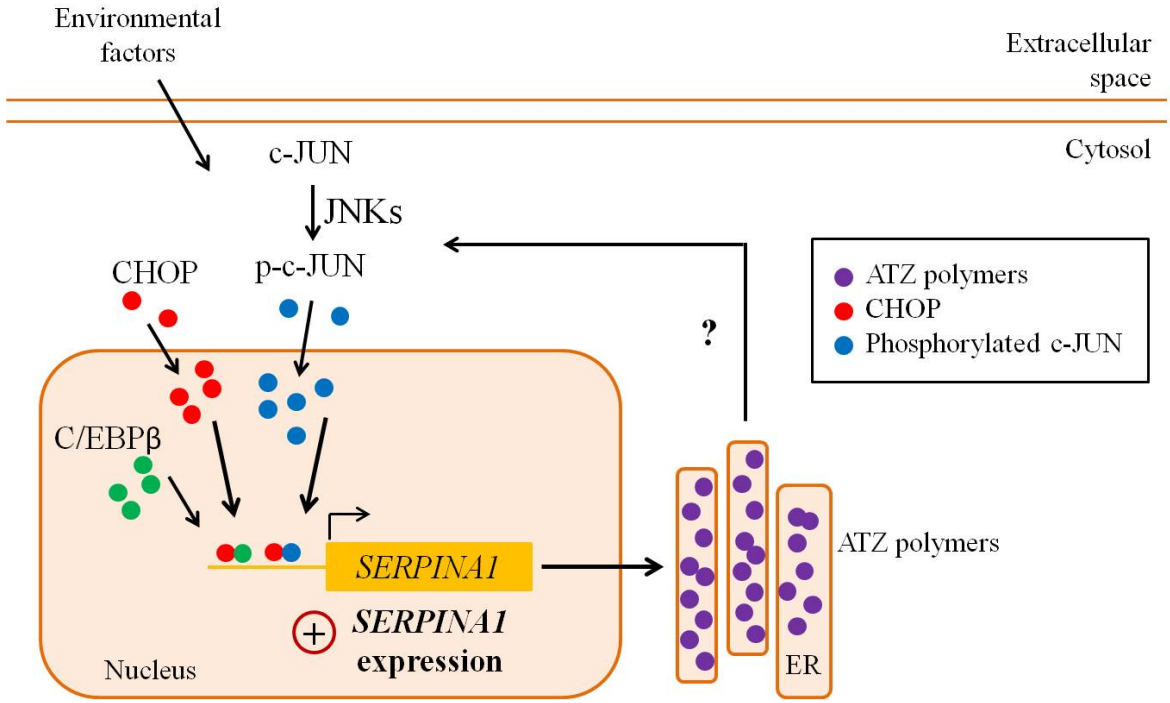

Figure 26: Graphical summary on the role of JNK and CHOP in the pathogenesis of liver disease due to ATZ.

Chapter 6: Bibliography

1. Sveger, T., The natural history of liver disease in alpha 1-antitrypsin deficient children. Acta Paediatr Scand, 1988. **77**(6): p. 847-51.
2. Laurell, C.B. and S. Eriksson, The Electrophoretic α;1-Globulin Pattern of Serum in α;1-Antitrypsin Deficiency. Scandinavian Journal of Clinical and Laboratory Investigation, 1963. **15**(2): p. 132-140.
3. Sharp, H.L., et al., Cirrhosis associated with alpha-1-antitrypsin deficiency: a previously unrecognized inherited disorder. J Lab Clin Med, 1969. **73**(6): p. 934-9.
4. de Serres, F.J., Worldwide racial and ethnic distribution of alpha1-antitrypsin deficiency: summary of an analysis of published genetic epidemiologic surveys. Chest, 2002. **122**(5): p. 1818-29.
5. Perlmutter, D.H., Alpha-1-antitrypsin deficiency: importance of proteasomal and autophagic degradative pathways in disposal of liver disease-associated protein aggregates. Annu Rev Med, 2011. **62**: p. 333-45.
6. de Serres, F.J., I. Blanco, and E. Fernandez-Bustillo, PI S and PI Z alpha-1 antitrypsin deficiency worldwide. A review of existing genetic epidemiological data. Monaldi Arch Chest Dis, 2007. **67**(4): p. 184-208.
7. Luisetti, M. and N. Seersholm, Alpha1-antitrypsin deficiency. 1: epidemiology of alpha1-antitrypsin deficiency. Thorax, 2004. **59**(2): p. 164-9.
8. Greene, C.M., et al., Alpha-1 antitrypsin deficiency: a conformational disease associated with lung and liver manifestations. J Inherit Metab Dis, 2008. **31**(1): p. 21-34.
9. Parr, D.G., et al., Pattern of emphysema distribution in alpha1-antitrypsin deficiency influences lung function impairment. Am J Respir Crit Care Med, 2004. **170**(11): p. 1172-8.
10. Morrison, H.M., et al., Lung lavage fluid from patients with alpha 1-proteinase inhibitor deficiency or chronic obstructive bronchitis: anti-elastase function and cell profile. Clin Sci (Lond), 1987. **72**(3): p. 373-81.
11. Hubbard, R.C., et al., Neutrophil accumulation in the lung in alpha 1-antitrypsin deficiency. Spontaneous release of leukotriene B4 by alveolar macrophages. J Clin Invest, 1991. **88**(3): p. 891-7.
12. Taggart, C., et al., Oxidation of either methionine 351 or methionine 358 in alpha 1-antitrypsin causes loss of anti-neutrophil elastase activity. J Biol Chem, 2000. **275**(35): p. 27258-65.
13. Larsson, C., Natural history and life expectancy in severe alpha1-antitrypsin deficiency, Pi Z. Acta Med Scand, 1978. **204**(5): p. 345-51.
14. Eriksson, S., J. Carlson, and R. Velez, Risk of cirrhosis and primary liver cancer in alpha 1-antitrypsin deficiency. N Engl J Med, 1986. **314**(12): p. 736-9.
15. Piitulainen, E., et al., Alpha1-antitrypsin deficiency in 26-year-old subjects: lung, liver, and protease/protease inhibitor studies. Chest, 2005. **128**(4): p. 2076-81.
16. Sveger, T., Liver disease in alpha1-antitrypsin deficiency detected by screening of 200,000 infants. N Engl J Med, 1976. **294**(24): p. 1316-21.
17. Pan, S., et al., Single nucleotide polymorphism-mediated translational suppression of endoplasmic reticulum mannosidase I modifies the onset of end-stage liver disease in alpha1-antitrypsin deficiency. Hepatology, 2009. **50**(1): p. 275-81.
18. Chu, A.S., K.B. Chopra, and D.H. Perlmutter, Is severe progressive liver disease caused by alpha-1-antitrypsin deficiency more common in children or adults? Liver Transpl, 2016. **22**(7): p. 886-94.
19. Su, W.P., et al., Alpha 1-antitrypsin deficiency panniculitis: a histopathologic and immunopathologic study of four cases. Am J Dermatopathol, 1987. **9**(6): p. 483-90.

20. Dowd, S.K., G.C. Rodgers, and J.P. Callen, Effective treatment with alpha 1-protease inhibitor of chronic cutaneous vasculitis associated with alpha 1-antitrypsin deficiency. J Am Acad Dermatol, 1995. **33**(5 Pt 2): p. 913-6.
21. Borawski, J., B. Naumnik, and M. Mysliwiec, Serum alpha1-antitrypsin but not complement C3 and C4 predicts chronic inflammation in hemodialysis patients. Ren Fail, 2003. **25**(4): p. 589-93.
22. Fagerhol, M.K. and C.B. Laurell, The polymorphism of "prealbumins" and alpha-1-antitrypsin in human sera. Clin Chim Acta, 1967. **16**(2): p. 199-203.
23. Salahuddin, P., Genetic variants of alpha1-antitrypsin. Curr Protein Pept Sci, 2010. **11**(2): p. 101-17.
24. Owen, M.C., et al., Mutation of antitrypsin to antithrombin. alpha 1-antitrypsin Pittsburgh (358 Met leads to Arg), a fatal bleeding disorder. N Engl J Med, 1983. **309**(12): p. 694-8.
25. Sifers, R.N., et al., A frameshift mutation results in a truncated alpha 1-antitrypsin that is retained within the rough endoplasmic reticulum. J Biol Chem, 1988. **263**(15): p. 7330-5.
26. Cox, D.W., V.D. Markovic, and I.E. Teshima, Genes for immunoglobulin heavy chains and for alpha 1-antitrypsin are localized to specific regions of chromosome 14q. Nature, 1982. **297**(5865): p. 428-30.
27. Morgan, K. and N.A. Kalsheker, Regulation of the serine proteinase inhibitor (SERPIN) gene alpha 1-antitrypsin: a paradigm for other SERPINs. Int J Biochem Cell Biol, 1997. **29**(12): p. 1501-11.
28. Perlino, E., R. Cortese, and G. Ciliberto, The human alpha 1-antitrypsin gene is transcribed from two different promoters in macrophages and hepatocytes. EMBO J, 1987. **6**(9): p. 2767-71.
29. Costa, R.H., D.R. Grayson, and J.E. Darnell, Jr., Multiple hepatocyte-enriched nuclear factors function in the regulation of transthyretin and alpha 1-antitrypsin genes. Mol Cell Biol, 1989. **9**(4): p. 1415-25.
30. Kalsheker, N., S. Morley, and K. Morgan, Gene regulation of the serine proteinase inhibitors alpha1-antitrypsin and alpha1-antichymotrypsin. Biochem Soc Trans, 2002. **30**(2): p. 93-8.
31. Aronsen, K.F., et al., Sequential changes of plasma proteins after surgical trauma. Scand J Clin Lab Invest Suppl, 1972. **124**: p. 127-36.
32. Knoell, D.L., et al., Alpha 1-antitrypsin and protease complexation is induced by lipopolysaccharide, interleukin-1beta, and tumor necrosis factor-alpha in monocytes. Am J Respir Crit Care Med, 1998. **157**(1): p. 246-55.
33. Carrell, R.W., et al., Structure and variation of human alpha 1-antitrypsin. Nature, 1982. **298**(5872): p. 329-34.
34. Brantly, M., T. Nukiwa, and R.G. Crystal, Molecular basis of alpha-1-antitrypsin deficiency. Am J Med, 1988. **84**(6A): p. 13-31.
35. Cichy, J., J. Potempa, and J. Travis, Biosynthesis of alpha1-proteinase inhibitor by human lung-derived epithelial cells. J Biol Chem, 1997. **272**(13): p. 8250-5.
36. Venembre, P., et al., Secretion of alpha 1-antitrypsin by alveolar epithelial cells. FEBS Lett, 1994. **346**(2-3): p. 171-4.
37. Geboes, K., et al., Morphological identification of alpha-I-antitrypsin in the human small intestine. Histopathology, 1982. **6**(1): p. 55-60.
38. Paakko, P., et al., Activated neutrophils secrete stored alpha 1-antitrypsin. Am J Respir Crit Care Med, 1996. **154**(6 Pt 1): p. 1829-33.
39. Cohen, A.B., Interrelationships between the human alveolar macrophage and alpha-1-antitrypsin. J Clin Invest, 1973. **52**(11): p. 2793-9.
40. Carrell, R.W., alpha 1-Antitrypsin: molecular pathology, leukocytes, and tissue damage. J Clin Invest, 1986. **78**(6): p. 1427-31.

41. Rao, N.V., et al., Characterization of proteinase-3 (PR-3), a neutrophil serine proteinase. Structural and functional properties. J Biol Chem, 1991. **266**(15): p. 9540-8.
42. Mast, A.E., et al., Analysis of the plasma elimination kinetics and conformational stabilities of native, proteinase-complexed, and reactive site cleaved serpins: comparison of alpha 1-proteinase inhibitor, alpha 1-antichymotrypsin, antithrombin III, alpha 2-antiplasmin, angiotensinogen, and ovalbumin. Biochemistry, 1991. **30**(6): p. 1723-30.
43. Bergin, D.A., et al., alpha-1 Antitrypsin regulates human neutrophil chemotaxis induced by soluble immune complexes and IL-8. J Clin Invest, 2010. **120**(12): p. 4236-50.
44. Janciauskiene, S., et al., Inhibition of lipopolysaccharide-mediated human monocyte activation, in vitro, by alpha1-antitrypsin. Biochem Biophys Res Commun, 2004. **321**(3): p. 592-600.
45. Libert, C., et al., alpha1-Antitrypsin inhibits the lethal response to TNF in mice. J Immunol, 1996. **157**(11): p. 5126-9.
46. Bergin, D.A., et al., The circulating proteinase inhibitor alpha-1 antitrypsin regulates neutrophil degranulation and autoimmunity. Sci Transl Med, 2014. **6**(217): p. 217ra1.
47. Lockett, A.D., et al., alpha(1)-Antitrypsin modulates lung endothelial cell inflammatory responses to TNF-alpha. Am J Respir Cell Mol Biol, 2013. **49**(1): p. 143-50.
48. Lomas, D.A., et al., The mechanism of Z alpha 1-antitrypsin accumulation in the liver. Nature, 1992. **357**(6379): p. 605-7.
49. Silverman, E.K. and R.A. Sandhaus, Clinical practice. Alpha1-antitrypsin deficiency. N Engl J Med, 2009. **360**(26): p. 2749-57.
50. Rudnick, D.A. and D.H. Perlmutter, Alpha-1-antitrypsin deficiency: a new paradigm for hepatocellular carcinoma in genetic liver disease. Hepatology, 2005. **42**(3): p. 514-21.
51. Lomas, D.A., et al., Polymerisation underlies alpha1-antitrypsin deficiency, dementia and other serpinopathies. Front Biosci, 2004. **9**: p. 2873-91.
52. Yamasaki, M., et al., Crystal structure of a stable dimer reveals the molecular basis of serpin polymerization. Nature, 2008. **455**(7217): p. 1255-8.
53. Yamasaki, M., et al., Molecular basis of alpha1-antitrypsin deficiency revealed by the structure of a domain-swapped trimer. EMBO Rep, 2011. **12**(10): p. 1011-7.
54. Miranda, E., et al., A novel monoclonal antibody to characterize pathogenic polymers in liver disease associated with alpha1-antitrypsin deficiency. Hepatology, 2010. **52**(3): p. 1078-88.
55. Kroeger, H., et al., Endoplasmic reticulum-associated degradation (ERAD) and autophagy cooperate to degrade polymerogenic mutant serpins. J Biol Chem, 2009. **284**(34): p. 22793-802.
56. Olzmann, J.A., R.R. Kopito, and J.C. Christianson, The mammalian endoplasmic reticulum-associated degradation system. Cold Spring Harb Perspect Biol, 2013. **5**(9).
57. Wang, H., et al., The ubiquitin ligase Hrd1 promotes degradation of the Z variant alpha 1-antitrypsin and increases its solubility. Mol Cell Biochem, 2011. **346**(1-2): p. 137-45.
58. Zhong, Y., et al., Identification of ERAD components essential for dislocation of the null Hong Kong variant of alpha-1-antitrypsin (NHK). Biochem Biophys Res Commun, 2015. **458**(2): p. 424-8.
59. Mizushima, N. and M. Komatsu, Autophagy: renovation of cells and tissues. Cell, 2011. **147**(4): p. 728-41.

60. Rubinsztein, D.C., G. Marino, and G. Kroemer, Autophagy and aging. Cell, 2011. **146**(5): p. 682-95.
61. Teckman, J.H. and D.H. Perlmutter, Retention of mutant alpha(1)-antitrypsin Z in endoplasmic reticulum is associated with an autophagic response. Am J Physiol Gastrointest Liver Physiol, 2000. **279**(5): p. G961-74.
62. Kamimoto, T., et al., Intracellular inclusions containing mutant alpha1-antitrypsin Z are propagated in the absence of autophagic activity. J Biol Chem, 2006. **281**(7): p. 4467-76.
63. Kruse, K.B., J.L. Brodsky, and A.A. McCracken, Characterization of an ERAD gene as VPS30/ATG6 reveals two alternative and functionally distinct protein quality control pathways: one for soluble Z variant of human alpha-1 proteinase inhibitor (A1PiZ) and another for aggregates of A1PiZ. Mol Biol Cell, 2006. **17**(1): p. 203-12.
64. Fregno, I., et al., ER-to-lysosome-associated degradation of proteasome-resistant ATZ polymers occurs via receptor-mediated vesicular transport. EMBO J, 2018. **37**(17).
65. Hidvegi, T., et al., Accumulation of mutant alpha1-antitrypsin Z in the endoplasmic reticulum activates caspases-4 and -12, NFkappaB, and BAP31 but not the unfolded protein response. J Biol Chem, 2005. **280**(47): p. 39002-15.
66. Hoesel, B. and J.A. Schmid, The complexity of NF-kappaB signaling in inflammation and cancer. Mol Cancer, 2013. **12**: p. 86.
67. Teckman, J.H., et al., Mitochondrial autophagy and injury in the liver in alpha 1-antitrypsin deficiency. Am J Physiol Gastrointest Liver Physiol, 2004. **286**(5): p. G851-62.
68. Haddock, C.J., et al., PiZ mouse liver accumulates polyubiquitin conjugates that associate with catalytically active 26S proteasomes. PLoS One, 2014. **9**(9): p. e106371.
69. Hidvegi, T., et al., Regulator of G Signaling 16 is a marker for the distinct endoplasmic reticulum stress state associated with aggregated mutant alpha1-antitrypsin Z in the classical form of alpha1-antitrypsin deficiency. J Biol Chem, 2007. **282**(38): p. 27769-80.
70. Ordonez, A., et al., Endoplasmic reticulum polymers impair luminal protein mobility and sensitize to cellular stress in alpha1-antitrypsin deficiency. Hepatology, 2013. **57**(5): p. 2049-60.
71. Lawless, M.W., et al., Activation of endoplasmic reticulum-specific stress responses associated with the conformational disease Z alpha 1-antitrypsin deficiency. J Immunol, 2004. **172**(9): p. 5722-6.
72. Wilson, A.A., et al., Emergence of a stage-dependent human liver disease signature with directed differentiation of alpha-1 antitrypsin-deficient iPS cells. Stem Cell Reports, 2015. **4**(5): p. 873-85.
73. Schmidt, B.Z. and D.H. Perlmutter, Grp78, Grp94, and Grp170 interact with alpha1-antitrypsin mutants that are retained in the endoplasmic reticulum. Am J Physiol Gastrointest Liver Physiol, 2005. **289**(3): p. G444-55.
74. Piccolo, P., et al., Down-regulation of hepatocyte nuclear factor-4alpha and defective zonation in livers expressing mutant Z alpha1-antitrypsin. Hepatology, 2017. **66**(1): p. 124-135.
75. Wewers, M.D. and R.G. Crystal, Alpha-1 antitrypsin augmentation therapy. COPD, 2013. **10 Suppl 1**: p. 64-7.
76. Wewers, M.D., et al., Replacement therapy for alpha 1-antitrypsin deficiency associated with emphysema. N Engl J Med, 1987. **316**(17): p. 1055-62.
77. Spencer, L.T., et al., Antibody response to aerosolized transgenic human alpha1-antitrypsin. N Engl J Med, 2005. **352**(19): p. 2030-1.

78. Petrache, I., J. Hajjar, and M. Campos, Safety and efficacy of alpha-1-antitrypsin augmentation therapy in the treatment of patients with alpha-1-antitrypsin deficiency. Biologics, 2009. **3**: p. 193-204.
79. Brantly, M.L., et al., Sustained transgene expression despite T lymphocyte responses in a clinical trial of rAAV1-AAT gene therapy. Proc Natl Acad Sci U S A, 2009. **106**(38): p. 16363-8.
80. Brantly, M.L., et al., Phase I trial of intramuscular injection of a recombinant adeno-associated virus serotype 2 alphal-antitrypsin (AAT) vector in AAT-deficient adults. Hum Gene Ther, 2006. **17**(12): p. 1177-86.
81. Flotte, T.R., et al., Phase 2 clinical trial of a recombinant adeno-associated viral vector expressing alpha1-antitrypsin: interim results. Hum Gene Ther, 2011. **22**(10): p. 1239-47.
82. Hidvegi, T., et al., An autophagy-enhancing drug promotes degradation of mutant alpha1-antitrypsin Z and reduces hepatic fibrosis. Science, 2010. **329**(5988): p. 229-32.
83. Kaushal, S., et al., Rapamycin reduces intrahepatic alpha-1-antitrypsin mutant Z protein polymers and liver injury in a mouse model. Exp Biol Med (Maywood), 2010. **235**(6): p. 700-9.
84. Pastore, N., et al., Gene transfer of master autophagy regulator TFEB results in clearance of toxic protein and correction of hepatic disease in alpha-1-anti-trypsin deficiency. EMBO Mol Med, 2013. **5**(3): p. 397-412.
85. Teckman, J.H., Lack of effect of oral 4-phenylbutyrate on serum alpha-1-antitrypsin in patients with alpha-1-antitrypsin deficiency: a preliminary study. J Pediatr Gastroenterol Nutr, 2004. **39**(1): p. 34-7.
86. Ordonez, A., et al., A single-chain variable fragment intrabody prevents intracellular polymerization of Z alpha1-antitrypsin while allowing its antiproteinase activity. FASEB J, 2015. **29**(6): p. 2667-78.
87. Bouchecareilh, M., et al., Histone deacetylase inhibitor (HDACi) suberoylanilide hydroxamic acid (SAHA)-mediated correction of alpha1-antitrypsin deficiency. J Biol Chem, 2012. **287**(45): p. 38265-78.
88. Mallya, M., et al., Small molecules block the polymerization of Z alpha1-antitrypsin and increase the clearance of intracellular aggregates. J Med Chem, 2007. **50**(22): p. 5357-63.
89. Guo, S., et al., Antisense oligonucleotide treatment ameliorates alpha-1 antitrypsin-related liver disease in mice. J Clin Invest, 2014. **124**(1): p. 251-61.
90. Sehgal, A., et al., 279 Pre-Clinical Evaluation of ALN-AAT to Ameliorate Liver Disease Associated With Alpha-1-Antitrypsin Deficiency. Gastroenterology, 2015. **148**(4): p. S-975.
91. Turner, A.M., et al., Hepatic-targeted RNA interference provides robust and persistent knockdown of alpha-1 antitrypsin levels in ZZ patients. J Hepatol, 2018.
92. Carlson, J.A., et al., Accumulation of PiZ alpha 1-antitrypsin causes liver damage in transgenic mice. J Clin Invest, 1989. **83**(4): p. 1183-90.
93. Dong, C., et al., Defective T cell differentiation in the absence of Jnk1. Science, 1998. **282**(5396): p. 2092-5.
94. Yang, D.D., et al., Differentiation of CD4+ T cells to Th1 cells requires MAP kinase JNK2. Immunity, 1998. **9**(4): p. 575-85.
95. Zinszner, H., et al., CHOP is implicated in programmed cell death in response to impaired function of the endoplasmic reticulum. Genes Dev, 1998. **12**(7): p. 982-95.
96. Gao, G.P., et al., Novel adeno-associated viruses from rhesus monkeys as vectors for human gene therapy. Proc Natl Acad Sci U S A, 2002. **99**(18): p. 11854-9.
97. Goodman, Z.D., Grading and staging systems for inflammation and fibrosis in chronic liver diseases. J Hepatol, 2007. **47**(4): p. 598-607.

98. Irizarry, R.A., et al., Exploration, normalization, and summaries of high density oligonucleotide array probe level data. Biostatistics, 2003. **4**(2): p. 249-64.
99. Gentleman, R.C., et al., Bioconductor: open software development for computational biology and bioinformatics. Genome Biol, 2004. **5**(10): p. R80.
100. Gautier, L., et al., affy--analysis of Affymetrix GeneChip data at the probe level. Bioinformatics, 2004. **20**(3): p. 307-15.
101. Baldi, P. and A.D. Long, A Bayesian framework for the analysis of microarray expression data: regularized t -test and statistical inferences of gene changes. Bioinformatics, 2001. **17**(6): p. 509-19.
102. Subramanian, A., et al., Gene set enrichment analysis: a knowledge-based approach for interpreting genome-wide expression profiles. Proc Natl Acad Sci U S A, 2005. **102**(43): p. 15545-50.
103. Han, J., et al., ER-stress-induced transcriptional regulation increases protein synthesis leading to cell death. Nat Cell Biol, 2013. **15**(5): p. 481-90.
104. B'Chir, W., et al., The eIF2alpha/ATF4 pathway is essential for stress-induced autophagy gene expression. Nucleic Acids Res, 2013. **41**(16): p. 7683-99.
105. Ma, D., S. Panda, and J.D. Lin, Temporal orchestration of circadian autophagy rhythm by C/EBPbeta. EMBO J, 2011. **30**(22): p. 4642-51.
106. Marcus, N.Y., et al., Characteristics of hepatocellular carcinoma in a murine model of alpha-1-antitrypsin deficiency. Hepatol Res, 2010. **40**(6): p. 641-53.
107. Giovannoni, I., et al., Alpha-1-antitrypsin deficiency: from genoma to liver disease. PiZ mouse as model for the development of liver pathology in human. Liver Int, 2015. **35**(1): p. 198-206.
108. Borel, F., et al., Editing out five Serpina1 paralogs to create a mouse model of genetic emphysema. Proc Natl Acad Sci U S A, 2018. **115**(11): p. 2788-2793.
109. Pastore, N., et al., Activation of the c-Jun N-terminal kinase pathway aggravates proteotoxicity of hepatic mutant Z alpha1-antitrypsin. Hepatology, 2017.
110. Leppa, S. and D. Bohmann, Diverse functions of JNK signaling and c-Jun in stress response and apoptosis. Oncogene, 1999. **18**(45): p. 6158-62.
111. Davis, R.J., Signal transduction by the JNK group of MAP kinases. Cell, 2000. **103**(2): p. 239-52.
112. Gupta, S., et al., Selective interaction of JNK protein kinase isoforms with transcription factors. EMBO J, 1996. **15**(11): p. 2760-70.
113. Krishna, M. and H. Narang, The complexity of mitogen-activated protein kinases (MAPKs) made simple. Cell Mol Life Sci, 2008. **65**(22): p. 3525-44.
114. Hess, J., P. Angel, and M. Schorpp-Kistner, AP-1 subunits: quarrel and harmony among siblings. J Cell Sci, 2004. **117**(Pt 25): p. 5965-73.
115. Karin, M., Z. Liu, and E. Zandi, AP-1 function and regulation. Curr Opin Cell Biol, 1997. **9**(2): p. 240-6.
116. Karin, M., The regulation of AP-1 activity by mitogen-activated protein kinases. J Biol Chem, 1995. **270**(28): p. 16483-6.
117. Pulverer, B.J., et al., Phosphorylation of c-jun mediated by MAP kinases. Nature, 1991. **353**(6345): p. 670-4.
118. Smeal, T., et al., Oncogenic and transcriptional cooperation with Ha-Ras requires phosphorylation of c-Jun on serines 63 and 73. Nature, 1991. **354**(6353): p. 494-6.
119. Bennett, B.L., et al., SP600125, an anthrapyrazolone inhibitor of Jun N-terminal kinase. Proc Natl Acad Sci U S A, 2001. **98**(24): p. 13681-6.
120. Derijard, B., et al., JNK1: a protein kinase stimulated by UV light and Ha-Ras that binds and phosphorylates the c-Jun activation domain. Cell, 1994. **76**(6): p. 1025-37.
121. Fornace, A.J., Jr., et al., Mammalian genes coordinately regulated by growth arrest signals and DNA-damaging agents. Mol Cell Biol, 1989. **9**(10): p. 4196-203.

122. Carlson, S.G., et al., Regulation of the C/EBP-related gene gadd153 by glucose deprivation. Mol Cell Biol, 1993. **13**(8): p. 4736-44.
123. Bruhat, A., et al., Amino acid limitation induces expression of CHOP, a CCAAT/enhancer binding protein-related gene, at both transcriptional and post-transcriptional levels. J Biol Chem, 1997. **272**(28): p. 17588-93.
124. Zheng, X., et al., Acute hypoxia induces apoptosis of pancreatic beta-cell by activation of the unfolded protein response and upregulation of CHOP. Cell Death Dis, 2012. **3**: p. e322.
125. Hetz, C., The unfolded protein response: controlling cell fate decisions under ER stress and beyond. Nat Rev Mol Cell Biol, 2012. **13**(2): p. 89-102.
126. Marciniak, S.J., et al., CHOP induces death by promoting protein synthesis and oxidation in the stressed endoplasmic reticulum. Genes Dev, 2004. **18**(24): p. 3066-77.
127. Chikka, M.R., et al., C/EBP homologous protein (CHOP) contributes to suppression of metabolic genes during endoplasmic reticulum stress in the liver. J Biol Chem, 2013. **288**(6): p. 4405-15.
128. DeZwaan-McCabe, D., et al., The stress-regulated transcription factor CHOP promotes hepatic inflammatory gene expression, fibrosis, and oncogenesis. PLoS Genet, 2013. **9**(12): p. e1003937.
129. Oyadomari, S. and M. Mori, Roles of CHOP/GADD153 in endoplasmic reticulum stress. Cell Death Differ, 2004. **11**(4): p. 381-9.
130. Yang, Y., et al., Transcription Factor C/EBP Homologous Protein in Health and Diseases. Front Immunol, 2017. **8**: p. 1612.
131. Fuchs, C.D., et al., FXR controls CHOP expression in steatohepatitis. FEBS Lett, 2017. **591**(20): p. 3360-3368.
132. Yoshida, H., et al., ATF6 activated by proteolysis binds in the presence of NF-Y (CBF) directly to the cis-acting element responsible for the mammalian unfolded protein response. Mol Cell Biol, 2000. **20**(18): p. 6755-67.
133. Lee, A.H., N.N. Iwakoshi, and L.H. Glimcher, XBP-1 regulates a subset of endoplasmic reticulum resident chaperone genes in the unfolded protein response. Mol Cell Biol, 2003. **23**(21): p. 7448-59.
134. Harding, H.P., et al., Regulated translation initiation controls stress-induced gene expression in mammalian cells. Mol Cell, 2000. **6**(5): p. 1099-108.
135. Guyton, K.Z., Q. Xu, and N.J. Holbrook, Induction of the mammalian stress response gene GADD153 by oxidative stress: role of AP-1 element. Biochem J, 1996. **314 (Pt 2)**: p. 547-54.
136. Wang, X.Z. and D. Ron, Stress-induced phosphorylation and activation of the transcription factor CHOP (GADD153) by p38 MAP Kinase. Science, 1996. **272**(5266): p. 1347-9.
137. Oyadomari, S., et al., Targeted disruption of the Chop gene delays endoplasmic reticulum stress-mediated diabetes. J Clin Invest, 2002. **109**(4): p. 525-32.
138. Song, B., et al., Chop deletion reduces oxidative stress, improves beta cell function, and promotes cell survival in multiple mouse models of diabetes. J Clin Invest, 2008. **118**(10): p. 3378-89.
139. Tamaki, N., et al., CHOP deficiency attenuates cholestasis-induced liver fibrosis by reduction of hepatocyte injury. Am J Physiol Gastrointest Liver Physiol, 2008. **294**(2): p. G498-505.
140. Toriguchi, K., et al., Attenuation of steatohepatitis, fibrosis, and carcinogenesis in mice fed a methionine-choline deficient diet by CCAAT/enhancer-binding protein homologous protein deficiency. J Gastroenterol Hepatol, 2014. **29**(5): p. 1109-18.
141. Marwarha, G., et al., Gadd153 and NF-kappaB crosstalk regulates 27-hydroxycholesterol-induced increase in BACE1 and beta-amyloid production in human neuroblastoma SH-SY5Y cells. PLoS One, 2013. **8**(8): p. e70773.

142. Kumar, R., et al., Brain ischemia and reperfusion activates the eukaryotic initiation factor 2alpha kinase, PERK. J Neurochem, 2001. **77**(5): p. 1418-21.
143. Milhavet, O., et al., Involvement of Gadd153 in the pathogenic action of presenilin-1 mutations. J Neurochem, 2002. **83**(3): p. 673-81.
144. Das, I., et al., Preventing proteostasis diseases by selective inhibition of a phosphatase regulatory subunit. Science, 2015. **348**(6231): p. 239-42.
145. Mueller, C., et al., Sustained miRNA-mediated knockdown of mutant AAT with simultaneous augmentation of wild-type AAT has minimal effect on global liver miRNA profiles. Mol Ther, 2012. **20**(3): p. 590-600.
146. Hubner, R.H., et al., Dysfunctional glycogen storage in a mouse model of alpha1-antitrypsin deficiency. Am J Respir Cell Mol Biol, 2009. **40**(2): p. 239-47.
147. Lindblad, D., K. Blomenkamp, and J. Teckman, Alpha-1-antitrypsin mutant Z protein content in individual hepatocytes correlates with cell death in a mouse model. Hepatology, 2007. **46**(4): p. 1228-35.
148. Ubeda, M., et al., Stress-induced binding of the transcriptional factor CHOP to a novel DNA control element. Mol Cell Biol, 1996. **16**(4): p. 1479-89.
149. Ubeda, M., M. Vallejo, and J.F. Habener, CHOP enhancement of gene transcription by interactions with Jun/Fos AP-1 complex proteins. Mol Cell Biol, 1999. **19**(11): p. 7589-99.
150. Chiribau, C.B., et al., Molecular symbiosis of CHOP and C/EBP beta isoform LIP contributes to endoplasmic reticulum stress-induced apoptosis. Mol Cell Biol, 2010. **30**(14): p. 3722-31.
151. Fawcett, T.W., et al., Physical and functional association between GADD153 and CCAAT/enhancer-binding protein beta during cellular stress. J Biol Chem, 1996. **271**(24): p. 14285-9.
152. Ron, D. and J.F. Habener, CHOP, a novel developmentally regulated nuclear protein that dimerizes with transcription factors C/EBP and LAP and functions as a dominant-negative inhibitor of gene transcription. Genes Dev, 1992. **6**(3): p. 439-53.
153. Seki, E., D.A. Brenner, and M. Karin, A liver full of JNK: signaling in regulation of cell function and disease pathogenesis, and clinical approaches. Gastroenterology, 2012. **143**(2): p. 307-20.
154. Boutten, A., et al., Oncostatin M is a potent stimulator of alpha1-antitrypsin secretion in lung epithelial cells: modulation by transforming growth factor-beta and interferon-gamma. Am J Respir Cell Mol Biol, 1998. **18**(4): p. 511-20.
155. Wang, A., et al., Transcription factor complex AP-1 mediates inflammation initiated by Chlamydia pneumoniae infection. Cell Microbiol, 2013. **15**(5): p. 779-94.
156. Guinea-Viniegra, J., et al., TNFalpha shedding and epidermal inflammation are controlled by Jun proteins. Genes Dev, 2009. **23**(22): p. 2663-74.
157. Carroll, T.P., et al., Evidence for unfolded protein response activation in monocytes from individuals with alpha-1 antitrypsin deficiency. J Immunol, 2010. **184**(8): p. 4538-46.
158. Hassan, T., et al., miR-199a-5p Silencing Regulates the Unfolded Protein Response in COPD and alpha1 Antitrypsin Deficiency. Am J Respir Crit Care Med, 2013.
159. Graham, K.S., A. Le, and R.N. Sifers, Accumulation of the insoluble PiZ variant of human alpha 1-antitrypsin within the hepatic endoplasmic reticulum does not elevate the steady-state level of grp78/BiP. J Biol Chem, 1990. **265**(33): p. 20463-8.
160. Ichijo, H., et al., Induction of apoptosis by ASK1, a mammalian MAPKKK that activates SAPK/JNK and p38 signaling pathways. Science, 1997. **275**(5296): p. 90-4.

161. Sakurai, T., et al., Loss of hepatic NF-kappa B activity enhances chemical hepatocarcinogenesis through sustained c-Jun N-terminal kinase 1 activation. Proc Natl Acad Sci U S A, 2006. **103**(28): p. 10544-51.
162. Hui, L., et al., p38alpha suppresses normal and cancer cell proliferation by antagonizing the JNK-c-Jun pathway. Nat Genet, 2007. **39**(6): p. 741-9.
163. Hui, L., et al., Proliferation of human HCC cells and chemically induced mouse liver cancers requires JNK1-dependent p21 downregulation. J Clin Invest, 2008. **118**(12): p. 3943-53.
164. Eferl, R., et al., Liver tumor development. c-Jun antagonizes the proapoptotic activity of p53. Cell, 2003. **112**(2): p. 181-92.
165. Malhi, H. and R.J. Kaufman, Endoplasmic reticulum stress in liver disease. J Hepatol, 2011. **54**(4): p. 795-809.
166. Fafournoux, P., A. Bruhat, and C. Jousse, Amino acid regulation of gene expression. Biochem J, 2000. **351**(Pt 1): p. 1-12.
167. Cazanave, S.C., et al., CHOP and AP-1 cooperatively mediate PUMA expression during lipoapoptosis. Am J Physiol Gastrointest Liver Physiol, 2010. **299**(1): p. G236-43.
168. Donato, L.J., et al., Reference and interpretive ranges for alpha(1)-antitrypsin quantitation by phenotype in adult and pediatric populations. Am J Clin Pathol, 2012. **138**(3): p. 398-405.
169. Lussier, B. and A.A. Wilson, Alpha-1 Antitrypsin: The Protein, in Alpha-1 Antitrypsin: Role in Health and Disease, A. Wanner and R.A. Sandhaus, Editors. 2016, Springer International Publishing: Cham. p. 17-30.
170. Tsutsumi, S., et al., Endoplasmic reticulum stress response is involved in nonsteroidal anti-inflammatory drug-induced apoptosis. Cell Death Differ, 2004. **11**(9): p. 1009-16.
171. Rudnick, D.A., et al., Indomethacin increases liver damage in a murine model of liver injury from alpha-1-antitrypsin deficiency. Hepatology, 2006. **44**(4): p. 976-82.
172. Gunawan, B.K., et al., c-Jun N-terminal kinase plays a major role in murine acetaminophen hepatotoxicity. Gastroenterology, 2006. **131**(1): p. 165-78.
173. Uzi, D., et al., CHOP is a critical regulator of acetaminophen-induced hepatotoxicity. J Hepatol, 2013. **59**(3): p. 495-503.
174. Updegraff, B.L. and K.A. O'Donnell, Stressing the importance of CHOP in liver cancer. PLoS Genet, 2013. **9**(12): p. e1004045.
175. Crozat, A., et al., Fusion of CHOP to a novel RNA-binding protein in human myxoid liposarcoma. Nature, 1993. **363**(6430): p. 640-4.
176. Rabbitts, T.H., et al., Fusion of the dominant negative transcription regulator CHOP with a novel gene FUS by translocation t(12;16) in malignant liposarcoma. Nat Genet, 1993. **4**(2): p. 175-80.
177. Perlmutter, D.H., Pathogenesis of chronic liver injury and hepatocellular carcinoma in alpha-1-antitrypsin deficiency. Pediatr Res, 2006. **60**(2): p. 233-8.